NASA TECHNICAL NOTE

NASA TN D-8137

NASA TN D-8137

THE PRODUCTION OF NITRIC OXIDE IN THE TROPOSPHERE AS A RESULT OF SOLID-ROCKET-MOTOR AFTERBURNING

Roger B. Stewart and Richard I. Gomberg

Langley Research Center
Hampton, Va. 23665

NATIONAL AERONAUTICS AND SPACE ADMINISTRATION • WASHINGTON, D. C. • MARCH 1976

1 Report No	2 Government Accession No	3 Recipient's Catalog No
NASA TN D-8137		

4 Title and Subtitle	5 Report Date
THE PRODUCTION OF NITRIC OXIDE IN THE TROPOSPHERE AS A RESULT OF SOLID-ROCKET-MOTOR AFTERBURNING	March 1976
	6 Performing Organization Code

7 Author(s)	8 Performing Organization Report No
Roger B. Stewart and Richard I. Gomberg	L-10594
	10 Work Unit No
	197-40-02-01

9 Performing Organization Name and Address	11 Contract or Grant No
NASA Langley Research Center Hampton, Va. 23665	

12 Sponsoring Agency Name and Address	13 Type of Report and Period Covered
National Aeronautics and Space Administration Washington, D.C. 20546	Technical Note
	14 Sponsoring Agency Code

15 Supplementary Notes

16 Abstract

As part of an ongoing assessment of the environmental effects of solid-rocket-motor operations in the troposphere, estimates are made of the nitric oxide produced in the troposphere by the space shuttle and Titan III-C boosters. The calculations made with the low-altitude plume program (LAPP) include the effects of coupled finite-rate chemistry and turbulent mixing. A recent measurement of nitric oxide taken in the effluent cloud of a Titan III-C booster is compared with calculations made with this computer code.

17 Key Words (Suggested by Author(s))	18 Distribution Statement
Environmental effects Space shuttle Troposphere pollution	Unclassified – Unlimited Subject Category 16

19 Security Classif (of this report)	20 Security Classif (of this page)	21 No of Pages	22 Price*
Unclassified	Unclassified	43	$3.75

*For sale by the National Technical Information Service, Springfield, Virginia 22161

THE PRODUCTION OF NITRIC OXIDE IN THE TROPOSPHERE AS A RESULT OF SOLID-ROCKET-MOTOR AFTERBURNING

Roger B. Stewart and Richard I. Gomberg
Langley Research Center

SUMMARY

As part of an ongoing assessment of the environmental effects of solid-rocket-motor operations in the troposphere, estimates are made of the nitric oxide produced in the troposphere by the space shuttle and Titan III-C boosters. The calculations made with the low-altitude plume program (LAPP) include the effects of coupled finite-rate chemistry and turbulent mixing. A recent measurement of nitric oxide taken in the effluent cloud of a Titan III-C booster is compared with calculations made with this computer code.

INTRODUCTION

The National Aeronautics and Space Administration is carrying out a continuing program of environmental assessment of the effects of solid-rocket-motor operations in the troposphere and stratosphere. The present study deals with the production of nitric oxide in the troposphere from space shuttle and Titan III-C solid rocket motors. Nitric oxide (NO) enters directly into the catalytic destruction of ozone in the stratosphere and, as such, presents a possible environmental hazard. (See ref. 1.) Calculations of the net production of NO from shuttle booster operations in the stratosphere are in progress. (See ref. 2.) The low-altitude production of NO is also of interest for comparison with ongoing tropospheric measurements (ref. 3) in order to give confidence in the plume modeling. At some intermediate altitude, the low-altitude NO results must be able to match smoothly the NO predictions of the stratospheric code for a given configuration.

The primary tool used in the investigation was the low-altitude plume program, the LAPP code. (See ref. 4.) This code can model a reacting, turbulent shear flow and is suitable for relatively low-altitude computational studies of NO production in rocket plumes. Above an altitude of 15 km, the rocket nozzle flow becomes increasingly under-expanded and a shock pattern develops in the plume that is not accounted for by the code. This report describes the use of the LAPP code and the computational studies carried out. In addition, recent measurements of NO made within a Titan III-C "ground cloud" by NASA Langley Research Center and Dr. D. Davis of the University of Maryland are described and a comparison is made between the measurements and model predictions.

SYMBOLS

A	area of plume
M	Mach number
p	pressure
R	effective nozzle exit radius (derived from true exit radius by means of an isentropic expansion)
R_g	universal gas constant
T	temperature
t	time in minutes
U	velocity of particle within plume
X	distance downstream of nozzle exit plane
Y	radial distance
ρ	density of plume
χ	concentration
$( )_{Al_2O_3}$	quantity appropriate to Al_2O_3

ANALYTICAL STUDIES

The LAPP Code

Figure 1 is a diagram of a typical low-altitude rocket plume assumed by the LAPP code. The LAPP code used in this study is an axisymmetric model that divides the hydrodynamic flow into stream tubes. The unperturbed atmosphere or free stream is the outermost stream tube; the remaining stream tubes comprise the plume. In each stream tube the governing differential equations are the reacting boundary-layer equations. (See ref. 5.) Finite-rate chemistry enters into the hydrodynamic description through the energy terms.

Several eddy-viscosity models are presently available which describe the turbulent entrainment of air into the plume. The Donaldson-Gray model (ref. 6) was used in this investigation because of its success in prior studies by other investigators (ref. 7).

As inputs to the code, it is necessary to specify the conditions at the nozzle exit plane, the conditions in the unperturbed atmosphere, the chemical reactions to be considered, and all the pertinent thermochemical data. The nozzle exit plane conditions for the space shuttle solid-rocket motor (SRM) were furnished by Marshall Space Flight Center and the data for the Titan III-C SRM by Aero-Space Corporation. (See tables I and II.) The unperturbed atmospheric conditions were taken from U.S. Standard Atmosphere (ref. 8), thermochemical data were taken from the JANAF reports (ref. 9), and chemical reaction rate coefficients were taken from references 2 and 10 to 14.

Because the reaction mechanism used in the code is not appropriate for temperatures below 600 K, the code cuts off all chemical kinetic reactions below this temperature. At tropospheric altitudes both the shuttle and Titan motors produce regions extending about 750 meters downstream of the nozzle exit plane in which temperatures are well above 600 K. The preponderance of NO is produced in these regions so that use of the LAPP code is appropriate here.

The chemical reactions and the rate coefficients used in this study are given in table III. These reactions are descriptive of processes occurring above 600 K. Certain species which react primarily at temperatures below this value are also considered and listed in table III. They are important for their thermodynamic properties. All constituents of the plume are taken to be ideal gases.

Modifications to LAPP Code

Three modifications were made to the LAPP code in the course of this study to improve on certain weaknesses in the original model. In order to study the overall effects of high-temperature chemical reactions, the plume calculations had to be carried to distances on the order of 750 meters downstream of the nozzle exit plane. Calculations to these distances have shown that mass is not conserved within the plume.

Consider, for example, figure 2 which shows the mass flow rate of the inert species Al_2O_3 plotted against downstream distance in the exhaust of a shuttle motor at an altitude of 15 km. Since Al_2O_3 is one of the inert species in the model, this quantity should be conserved. If X is the distance downstream, the mass flow rate of Al_2O_3 is $(\rho UA)_{Al_2O_3}$ and should be constant for all X. As can be seen in figure 2, the quantity is actually decreasing with downstream distance because mass is being lost. The mass loss is caused by the failure of the model to account adequately for the expansion of the plume. The model expands the plume by adding stream tubes whenever the temperature of second

to outermost stream tube T_{n-1} and the outermost tubes temperature T_n satisfy $\frac{|T_n - T_{n-1}|}{|T_n|} > 0.050$. At distances far downstream of the exit plane, where the mass loss occurs, this criterion does not allow enough stream tubes to be added for sufficient expansion to occur. As a result, the species found in the plume but not in the atmosphere are truncated at the free atmosphere boundary and mass is lost.

Pergament and Thorpe (ref. 2) have suggested an empirical scheme which corrects for this deficiency. Their method, which is used in the present study, is essentially to normalize the mass flow of all species at a given downstream distance by the ratio of the Al_2O_3 mass flow at that same distance to the mass flow of Al_2O_3 at the exit plane. Their studies indicate that this is a satisfactory approach.

Another problem encountered in using the LAPP code is a continuation error. For complicated chemistry the computer time required for a given problem can be several hours. Because of computer scheduling, it is practical to run only part of the problem at a time, punch out a continuation deck, and resubmit this deck at a later time. Indeed, this is an option in the LAPP code. However, for each new deck, the code's boundary conditions force the second to the outermost stream tube to be identical to the outermost stream tube which is the unperturbed atmosphere. Any compounds such as Al_2O_3, NO, or NO_2 not found in the atmosphere are deleted from the tube and this deletion introduces a small error each time the problem is "continued." If many continuations are made, the cumulative differences can become large as seen in figure 3.

The center-line temperature is plotted as a function of distance downstream of the exit plane for a Titan motor at an altitude of 1.2 km in figure 3. If one, two, or three continuations are used, the profile shown with the solid line results; the three cases are indistinguishable. For 28 continuations, the profile is changed as shown by the dashed line though identical inputs were used. To avoid this spurious effect, all cases used in this study were run by using three or less continuations.

At high altitudes when the pressure of the gases at the exit plane is on the order of 1 atmosphere, whereas the ambient pressure is about 0.1 atmosphere, there are very few collisions involving the plume gases as they stream out of the nozzle until they reach a pressure match with the atmosphere. For these high altitudes a hand-calculated isentropic expansion is used to gain effective nozzle exit plane conditions. This approach was used for the shuttle motor at altitudes of 5 and 15 km and for the Titan motors at 5 and 18 km. The chemical composition at the effective nozzle exit plane was assumed to be identical to those in tables I and II. By use of the mass flow rates taken from reference 15, those furnished by Battelle Columbus Laboratories, and the isentropic assumption, the complete set of effective exit plane conditions necessary to start the code at these higher altitudes is given in table IV.

Results

Calculations were made for a Titan solid-propellant booster at altitudes of 1.2, 5, and 18 km and for a shuttle motor at altitudes of 0.7, 5, and 15 km. The calculations neglect the shock structure present in the plume at very high altitudes and introduce some uncertainties in the 15- and 18-km cases. With increasing X/R, the temperatures in the plume decrease, the chemical reactions begin to slow down, and the velocities decrease. As X/R approaches the value where the center-line temperature drops below 600 K, an asympotic state is assumed. At a given X/R in this "asymptotic" region, a 1-meter-long section of plume in the X-direction contains a certain number of grams of NO, NO_2, Al_2O_3, and so on. Knowing the number of grams of NO per meter of plume in the X-direction in this slowly varying region is a reasonable indication of how much NO will be transferred from the afterburning region to that part of the plume for which temperatures are below 600 K.

In figure 4 the NO produced in a Titan solid-booster plume at three altitudes is shown. At 1.2 km, the amount of NO transferred to the cool part of the plume will be about 550 g/m for each motor, at 5 km it will be about 50 g/m for each motor, and at 18 km, 33 g/m for each motor. Since there are two solid boosters for a Titan III-C vehicle, and since at tropospheric altitudes there is very little interaction between the plumes, the total amounts of NO transferred from the afterburning region of the Titan are twice these numbers.

A similar analysis is carried out for a shuttle booster in figure 5. As can be seen, the asymptotic value of the shuttle motor at 0.7 km is about 900 g/m of NO for each motor, at 5 km it is 70 g/m of NO for each motor, and at 15 km, less than 11 g/m for each motor.

It is surprising that in spite of the fact that the mass flow rate of the space shuttle is twice that of a Titan, its high altitude production of NO is less than half of that of the Titan. The reason for this anomalous behavior of the NO production curve is the presence of a thrust vector control (TVC) system in the Titan which is not present in the shuttle. The Titan motor contains a set of jets which inject streams of N_2O_4 into the nozzle flow. These injectors are used to make fine course corrections in the booster ascent. At the high temperatures in the nozzle, much of this fluid breaks down into NO. As a conservative estimate for computational purposes, it is reasonable to assume that all of the fluid breaks down into NO and O_2. This assumption is made in the second column of table II.

In figure 6 the mole fraction of NO and other species along the plume center line of a Titan at 18 km is plotted as a function of the dimensionless downstream distance X/R. The NO mole fraction drops from its initial value as the plume expands and entrains air, steadies off as the chemical afterburning produces enough NO to compensate for the plume

dilution, and finally drops as the reactions slow and dilution becomes dominant. In figure 7 the same plot is made, the NO produced by the thrust vector control (TVC) system being neglected. The afterburning peak still brings the mole fraction up to a reasonably large value at X/R = 100, but clearly the TVC results in substantial contribution of NO. Figure 8 shows the amount of NO in grams per meter for the Titan at 18 km with TVC. Figure 9, without TVC, again reflects the importance of this additional NO.

Figures 10 to 14 describe various aspects of the Titan plume at 1.2 km. Figure 10 shows the fall off of CO as it afterburns to produce CO_2. Figure 11 follows the production of NO and other nitrogen and oxygen species. Figure 12 traces the production of several important afterburning products, and figures 13 and 14 show the development of the cross-sectional temperature and velocity profiles at various downstream stations.

A similar set of curves is shown for the Titan at 5 km in figures 15 and 16. The NO mole fraction plotted against dimensionless downstream distance (fig. 15) shows the double peak which seems to be characteristic of the Titan. The NO resulting from TVC is dominant at X/R near zero, whereas a second contribution results at X/R = 100 from the chemical afterburning. As shown in figure 16, combustion proceeds much as in the 1.2-km case. The temperature and velocity profiles are similar to the 1.2-km case and are not presented.

The center-line mole fraction profile of NO as a function of X/R in the shuttle motor differs significantly from that of the Titan. Profiles for NO and other nitrogen species mole fractions for the 0.7-km shuttle motor are plotted in figure 17. Note, in particular, that the NO mole fraction starts out at an extremely small value, in contrast to the Titan cases, but reaches a high level at X/R = 60 as a result of afterburning. This behavior is followed closely at higher altitudes as shown in figures 18 and 19, where the same profiles are presented for the 5- and 15-km shuttle motors. Note that for the 15-km shuttle case, the afterburning NO production reaches a peak at X/R = 90. Because of the lower densities at this altitude than at 0.7 km, the processes are "stretched out" over a longer distance and time.

The combustion of CO to CO_2 for the shuttle, on the other hand, is similar to that for the Titan. In figure 20 the center-line mole fractions of various combustible materials in the 0.7-km shuttle case show little qualitative difference between this case and the Titan case at 1.2 km. For the 15-km altitude shuttle case (fig. 21), the same comments apply, although the "stretching out" process still occurs.

Consider now figures 22 and 23, the velocity and temperature profiles for the 0.7-km shuttle. Comparison with figures 13 and 14 show strong similarities between these curves and those for the Titan at a similar altitude. In figures 24 and 25, the velocity and temperature profiles are presented at various downstream stations for the

shuttle solid-rocket motor at a 15-km altitude. Note again that the major difference between this case and the 0.7-km shuttle case is the slower rate of change as a function of X/R.

MEASUREMENTS

At the present time there are no measurements available for the production of effluents from the full-scale space shuttle boosters. As a general approach toward comparison of the plume calculations and measured production of chemical species, Titan III-C solid boosters have been selected as test vehicles. The Titan III-C booster motors are of similar chemical composition to the shuttle boosters and have about one-half the mass flow rate of the shuttle boosters.

After a Titan III-C launch in May 1974 at John F. Kennedy Space Center, a series of ground cloud penetrations were made with an instrumented aircraft under the Langley Research Center launch vehicle effluent monitoring program. The comparisons between the plume code predictions and measurements within the cloud were made by use of the following techniques. The ground cloud volume as a function of time was calculated by using visible photographs of the cloud from three separate camera sites. By using the known cloud position, the cloud images were divided into elliptical slabs and the volume was calculated. The Titan III trajectory and motor mass flow rate are then known functions of time so that by using time-sequenced visible spectrum photographs, the total amount of exhaust material in the ground cloud can be calculated.

Figure 26 is a plot of the Titan III-C ground cloud volume as a function of time following the May 20, 1974 launch at Kennedy Space Center. The cloud volume was obtained by using the technique described previously. The calculations were repeated with a different camera site location and the resulting calculated volume is also shown in figure 26 as the curve of the lower volume plotted against time. Figure 27 indicates the total mass in the cloud and shows several mass dilution ratios at different times.

The aircraft used for the cloud measurements was an instrumented Cessna 402. This aircraft made eight penetrations of the cloud and sampled the gaseous NO and NO_2 by using a commercially available $NO\text{-}NO_2\text{-}NO_x$ analyzer. The response time of the instrument is within a second. It can measure concentration as low as 5 parts per billion with an accuracy within 10 percent.

Ozone was also measured during the aircraft penetrations. Again, a commercially available instrument was used, in this case, a chemiluminescent ozone detector. It can measure concentration to 5 parts per billion with a response time of 1 second.

Figure 28 shows the data traces for NO and O_3 taken during two of the eight penetrations of the cloud by the aircraft. It is clear that the cloud is rather well mixed up to t + 34 minutes at which time the aircraft discontinued cloud penetration.

Figure 29 is a plot of the nondimensional cloud volume growth as a function of time and also the nondimensional NO concentration decay as a function of time. Figure 29 indicates that up to about t + 20 minutes, the decay in NO concentration closely follows the cloud volume growth Figures 26 to 29 include data obtained in cooperation with the University of Maryland.

An interesting comparison between the code's prediction and the aircraft's measurements can be made. Photographic data show that the exhaust ground cloud is made up of approximately 1.5 km of rocket plume. By assuming that 1500 m of the Titan plume near sea level will contain 1500 times the asymptotic value of NO in g/m of the Titan at 1.2 km, the total mass of NO at time of launch is known. Converting this quantity to the equivalent number of NO molecules and dividing by the cloud volume at a given time gives a number density at a given time. At 5 minutes, the time of the first aircraft penetration, this density is 700 parts per billion.

The aircraft data also furnish a number density for both NO and NO_2 (about 600 parts per billion of total NO_x). If it is assumed that all the NO and NO_2 measured by the aircraft resulted from the NO produced in the plume, the two values can be compared. The agreement (which is probably fortuitous) is within 20 percent.

SUMMARY OF RESULTS

The amount of nitric oxide NO produced in the afterburning region of the shuttle and Titan III-C solid rocket motors varies with altitude. For the first 10 km of altitude, the motor of the shuttle will produce more NO through afterburning than the Titan III-C motor. However, because of the existence of a vector thrust control system in the Titan III-C, at altitudes between 10 and 15 km, the Titan III-C solid-rocket motor produces more NO than the much larger shuttle motor which has no thrust vector control system. Experimental data taken by an aircraft at low altitudes compare closely with computer model's predictions within the assumptions of the comparison between theory and experiment.

Langley Research Center
National Aeronautics and Space Administration
Hampton, Va. 23665
January 29, 1976

REFERENCES

1. Kellogg, W. W.: Pollution of the Upper Atmosphere by Rockets. Space Sci. Rev., vol. III, no. 2, Aug. 1964, pp. 275-316.

2. Pergament, Harold S.; and Thorpe, Roger D.: NO_x Deposited in the Stratosphere by the Space Shuttle. AeroChem TN-161 (Contract NAS 1-13544), AeroChem Res. Labs., Inc., July 1975. (Available as NASA CR-132715.)

3. Gregory, Gerald L.; and Storey, Richard W., Jr.: Effluent Sampling of Titan III C Vehicle Exhaust. NASA TM X-3228, 1975.

4. Pergament, H. S.; and Calcote, H. F.: Thermal and Chemi-Ionization Processes in Afterburning Rocket Exhausts. Eleventh Symposium (International) on Combustion, Combustion Inst. (Pittsburgh, Pa.), 1967, pp. 597-611.

5. Vincenti, Walter G.; and Kruger, Charles H., Jr.: Introduction to Physical Gas Dynamics, John Wiley & Sons, Inc., c.1965.

6. Donaldson, Coleman duP.; and Gray, K. Evan: Theoretical and Experimental Investigation of the Compressible Free Mixing of Two Dissimilar Gases. AIAA J., vol. 4, no. 11, Nov. 1966, pp. 2017-2025.

7. Pergament, H. S.; and Mikatarian, R. R.: Calculation of Nonequilibrium Nozzle and Exhaust Plume Properties for Saturn Launch Vehicles. AeroChem TP-160, AeroChem Res. Labs., Inc., Aug. 1967. (Available as NASA CR-61704.)

8. U.S. Standard Atmosphere, 1962; NASA, U.S. Air Force, and U.S. Weather Bur., Dec. 1962.

9. JANAF Thermochemical Tables. Second ed., NSRDS-NBS 37, U.S. Dep. Com., June 1971.

10. Pergament, H. S.; and Jensen, D. E.: Influence of Chemical Kinetic and Turbulent Transport Coefficients on Afterburning Rocket Plumes. J. Spacecraft & Rockets, vol. 8, no. 6, June 1971, pp. 643-649.

11. Jensen, D. E.; and Jones, G. A.: Gas-Phase Reaction Rate Coefficients for Rocketry Applications. RPE-TR-71/9, Rocket Propulsion Establishment (Westcott, England), Oct. 1971.

12. Garvin, David; and Hampson, R. F., eds.: Chemical Kinetics Data Survey VII. Tables of Rate and Photochemical Data for Modelling of the Stratosphere (Revised). NBSIR 74-430, Nat. Bur. Standards, U.S. Dep. Com., Jan. 1974. (Supersedes NBSIR 73-203.)

13. Garvin, David, ed.: Chemical Kinetics Data Survey V. Sixty-Six Contributed Rate and Photochemical Data Evaluations on Ninety-Four Reactions. NBSIR 73-206, Nat. Bur. Standards, U.S. Dep. Com., May 1973.

14. Bowman, Craig T.: Investigation of Nitric Oxide Formation Kinetics in Combustion Processes: The Hydrogen-Oxygen-Nitrogen Reaction. Combust. Sci. & Technol., vol. 3, no. 1, Apr. 1971, pp. 37-45.

15. Solid Propellant Engineering Staff: Nozzle Exit Exhaust Products From Space Shuttle Boost Vehicle (November 1973 Design). Tech. Memo. 33-712, Jet Propulsion Lab., California Inst. Technol., Feb. 1975. (Available as NASA CR-136747.)

TABLE I.- SPACE SHUTTLE SOLID-ROCKET EXIT PLANE MOTOR AVERAGE VALUES

[Space shuttle data obtained from Ben Shackleford, Marshall Space Flight Center, Mar. 1974. These data are appropriate for altitudes less than 1 km]

Exit plane species	Mole fractions	Exit plane species	Mole fractions
AlCl	3×10^{-5}	H_2	$27\,812 \times 10^{-5}$
$AlCl_2$	8	H_2O	14 068
$AlCl_3$	1	NO	1
AlOCl	2	N_2	8 401
Al_2O_3	7 975	O	1
CO	23 205	OH	46
CO_2	2 120	ClO	8.1×10^{-9}
Cl	225	Cl_2	6.9×10^{-7}
Fe	11	HO_2	1.2×10^{-11}
FeCl	1	NO_2	5.8×10^{-12}
$FeCl_2$	122	N_2O	8.6×10^{-11}
H	556	O_2	2.0×10^{-7}
HCl	15 442	N	0.0

Exit plane conditions based on an equilibrium model:

p_{exit}, atm	0.8345
T_{exit}, K	2308
M_{exit}	2.779
R_{exit}, m	1.810
U_{exit}, m/s	2433.8

TABLE II.- TITAN MOTOR DATA

[These data are based on an equilibrium model and are appropriate for altitudes of approximately 1 km; in column three it is assumed that the injected N_2O_4 breaks down into NO and O_2]

Exit plane species	Without TCV	With TCV (based on 50 lb/sec per motor)
CO	2.468×10^{-1}	2.452×10^{-1}
OH	9.000×10^{-5}	9.000×10^{-5}
CO_2	1.811×10^{-2}	1.811×10^{-2}
H	3.200×10^{-3}	3.200×10^{-3}
O_2	1.035×10^{-3}	1.034×10^{-3}
HO_2	5.858×10^{-11}	5.585×10^{-11}
H_2	3.157×10^{-1}	3.136×10^{-1}
H_2O	1.058×10^{-1}	1.051×10^{-1}
NO	9.000×10^{-5}	6.680×10^{-3}
NO_2	2.002×10^{-11}	2.002×10^{-11}
N	1.884×10^{-8}	1.884×10^{-8}
N_2	8.105×10^{-2}	8.051×10^{-2}
HCl	1.510×10^{-1}	1.500×10^{-1}
N_2O	1.090×10^{-8}	1.090×10^{-8}
Cl	1.150×10^{-3}	1.150×10^{-3}
Cl_2	3.293×10^{-6}	3.293×10^{-6}
ClO	2.392×10^{-8}	2.392×10^{-8}
Al_2O_3	7.680×10^{-2}	7.170×10^{-2}
O	6.959×10^{-7}	6.959×10^{-7}

Exit plane conditions:

Mass flow at exit, g/sec . . . . . 1.84×10^6

T_{exit}, K 1921

p_{exit}, atm 0.702

R_{exit}, m 1.35

TABLE III.- CHEMICAL SCHEME [a]

Reaction	Rate coefficient
(1) $H + Cl + M = HCl + M$	$3 \times 10^{-29} T^{-1}$
(2) $H + HCl = Cl + H_2$	$8.8 \times 10^{-11} \exp(-4\,622/R_g T)$
(3) $HCl + OH = H_2O + Cl$	$7.2 \times 10^{-12} \exp(-3\,250/R_g T)$
(4) $H + H + M = H_2 + M$	$1 \times 10^{-29} T^{-1}$
(5) $H + OH + M = H_2O + M$	$1 \times 10^{-28} T^{-1}$
(6) $OH + OH = H_2O + O$	$1 \times 10^{-11} \exp(-1\,000/R_g T)$
(7) $OH + H_2 = H_2O + H$	$4 \times 10^{-11} \exp(-5\,500/R_g T)$
(8) $CO + OH = CO_2 + H$	$5 \times 10^{-13} \exp(-600/R_g T)$
(9) $O + O + M = O_2 + M$	$1 \times 10^{-29} T^{-1}$
(10) $CO + O + M = CO_2 + M$	$5 \times 10^{-29} T^{-1} \exp(-4\,000/R_g T)$
(11) $O + H_2 = OH + H$	$3 \times 10^{-11} \exp(-8\,200/R_g T)$
(12) $H + O_2 = OH + O$	$3 \times 10^{-10} \exp(-16\,500/R_g T)$
(13) $O + H + M = OH + M$	$1 \times 10^{-29} T^{-1}$
(14) $O + N_2 = NO + N$	$2.3 \times 10^{-10} \exp(-75\,400/R_g T)$
(15) $N + O_2 = NO + O$	$1.1 \times 10^{-14} T \exp(-6\,250/R_g T)$
(16) $NO + O + M = NO_2 + M$	$4.17 \times 10^{-33} \exp(+1\,860/R_g T)$
(17) $NO + OH = NO_2 + H$	$2.8 \times 10^{-12} \exp(-30\,000/R_g T)$
(18) $Cl + OH = HCl + O$	$3.0 \times 10^{-11} \exp(-9\,900/R_g T)$
(19) $Cl + Cl + M = Cl_2 + M$	$1.6 \times 10^{-33} \exp(+1\,600/R_g T)$

[a] Rate coefficient units are in terms of molecules, cm^3, sec. AlCl, $AlCl_2$, and Al_2O_3 are included in the plume as inert species. Coefficients for reactions 1 and 4 to 13 are from reference 10; reactions 2 and 3, from reference 2; reactions 14 and 15, from reference 14; reactions 16 and 17, from reference 13; and reactions 18 and 19 from reference 11. The rate coefficients from reactions 16, 18, and 19 were modified slightly from the values given in the references after discussions with Dr. H. Hoshizaki of Lockheed Aircraft Corporation.

TABLE IV.- TEST CONDITIONS

(a) Ambient conditions

	Ambient pressure, atm	Ambient temperature, K	Free-stream velocity, m/sec
Sea-level Titan	0.702	300	30.48
5-km Titan	.536	260	275.8
18-km Titan	.0797	207	537.6
Sea-level shuttle	.8345	300	30.48
5-km shuttle	.536	260	259.3
15-km shuttle	.119	216	552.2

(b) Exit plane conditions

	Effective exit radius, m	Effective exit temperature, K	Effective exit velocity, m/sec
Sea-level Titan	1.35	1921	2501
5-km Titan	1.35	1921	2501
18-km Titan	3.63	1375	3496
Sea-level shuttle	1.81	2308	2433
5-km shuttle	1.81	2308	2433
15-km shuttle	3.56	1726	2864

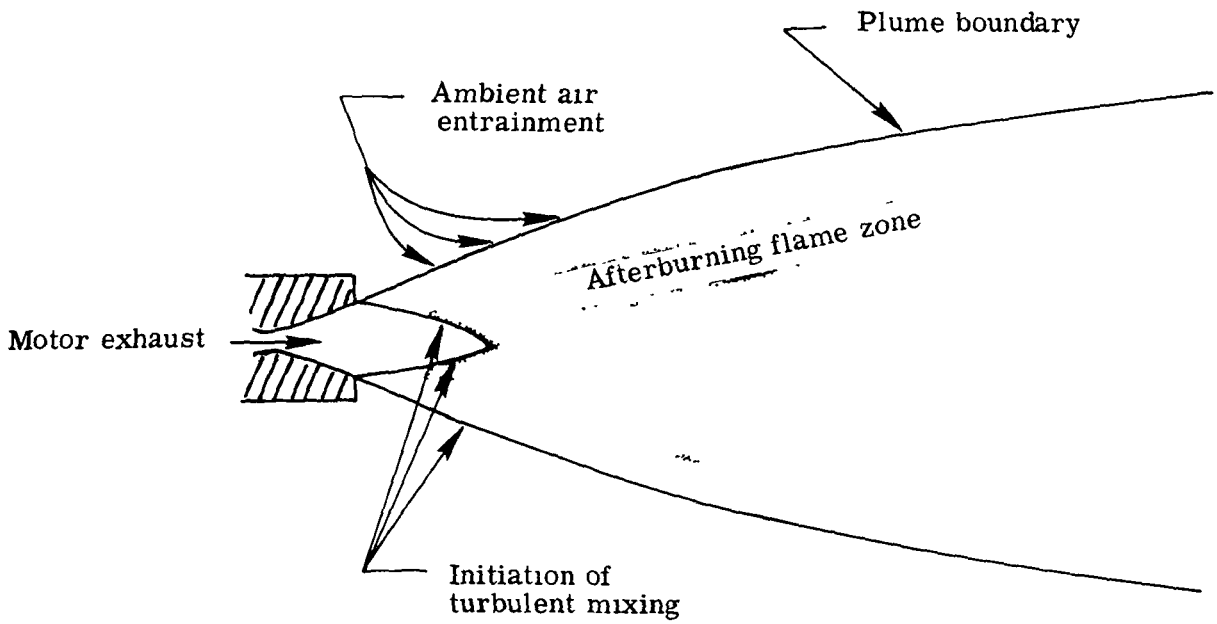

Figure 1.- Diagram of plume during tropospheric afterburning.

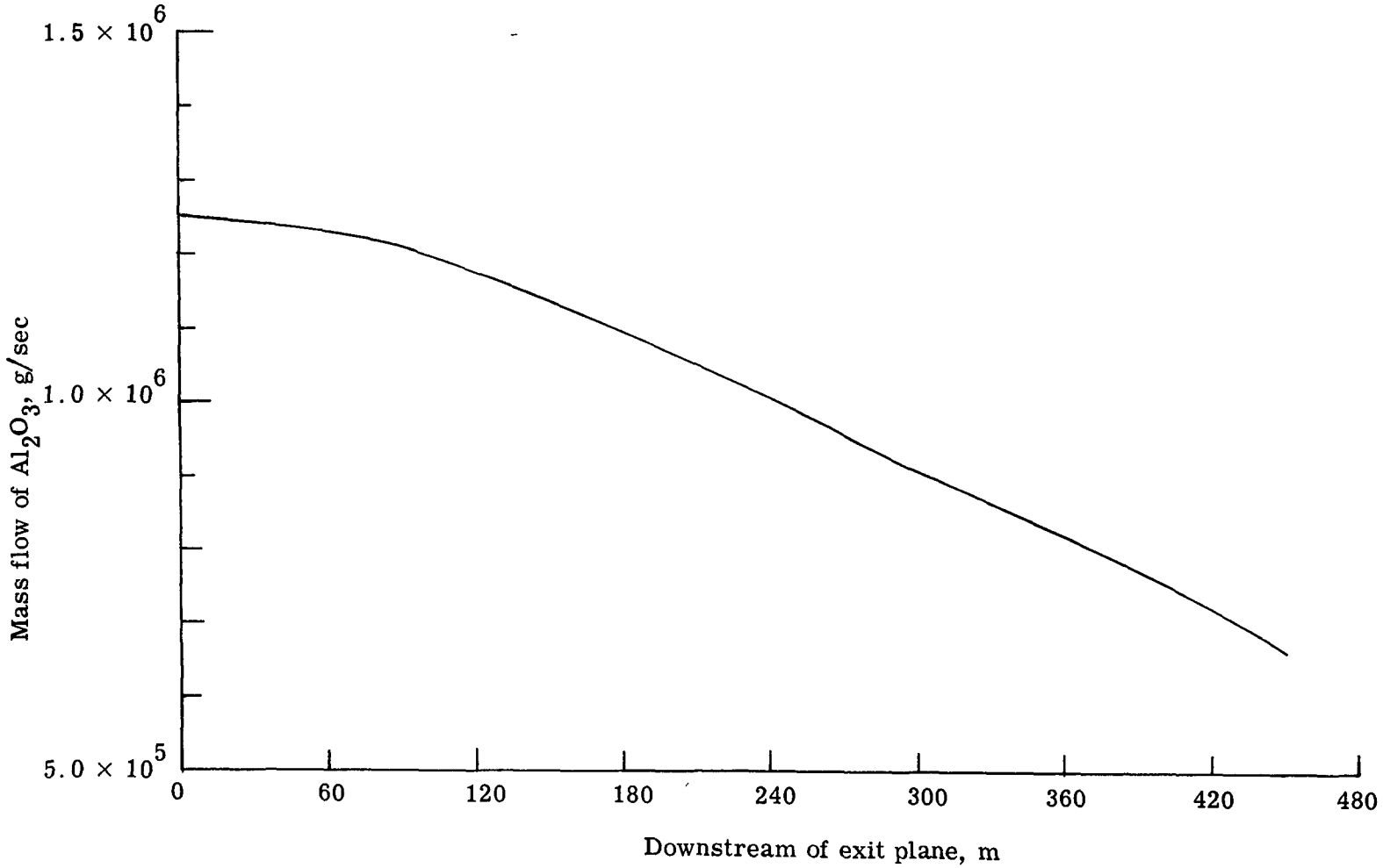

Figure 2.- Al_2O_3 mass flow in plume of a 15-km shuttle motor.

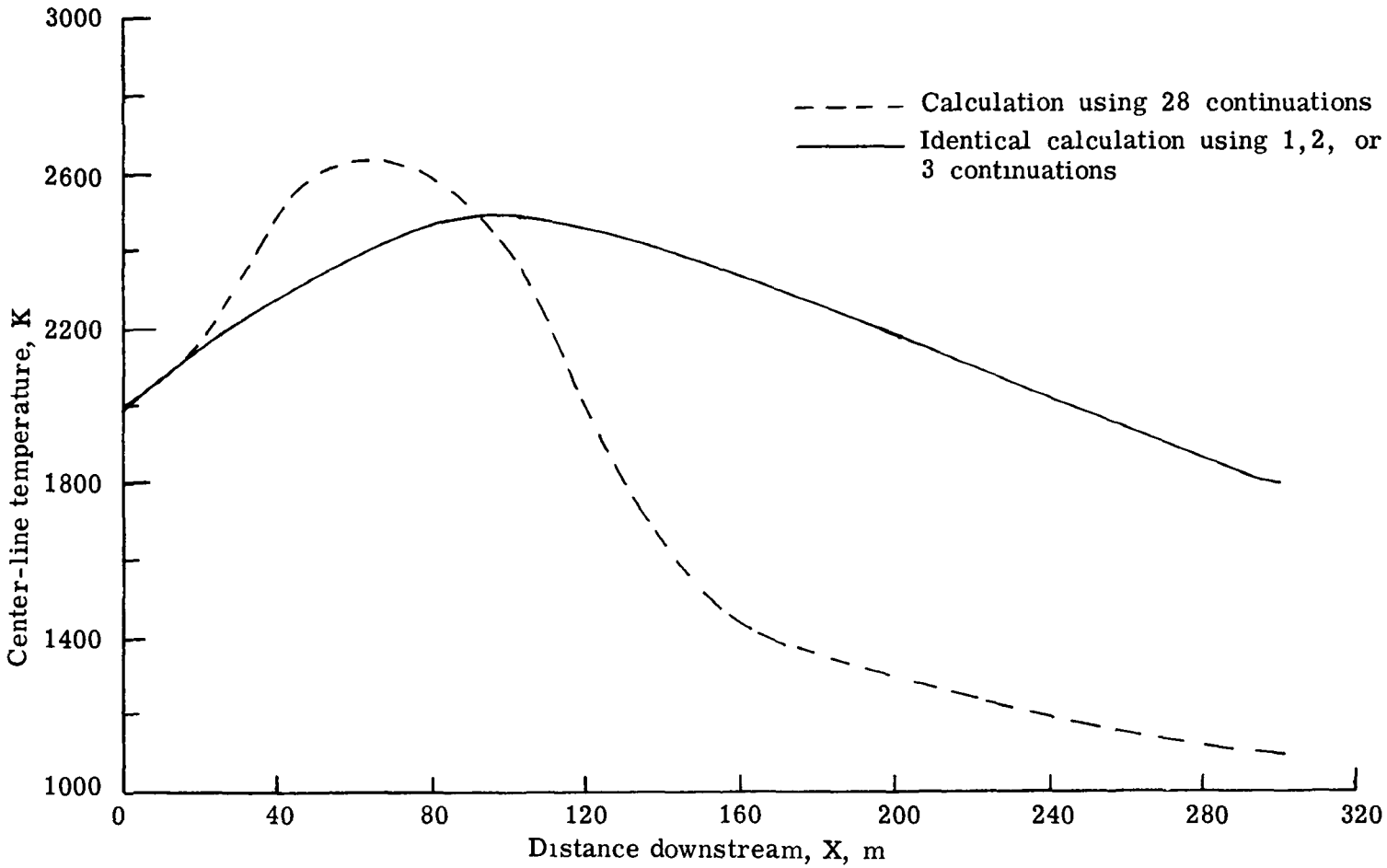

Figure 3.- Temperature profiles for plume of a Titan III-C motor at 18 km for various numbers of continuations.

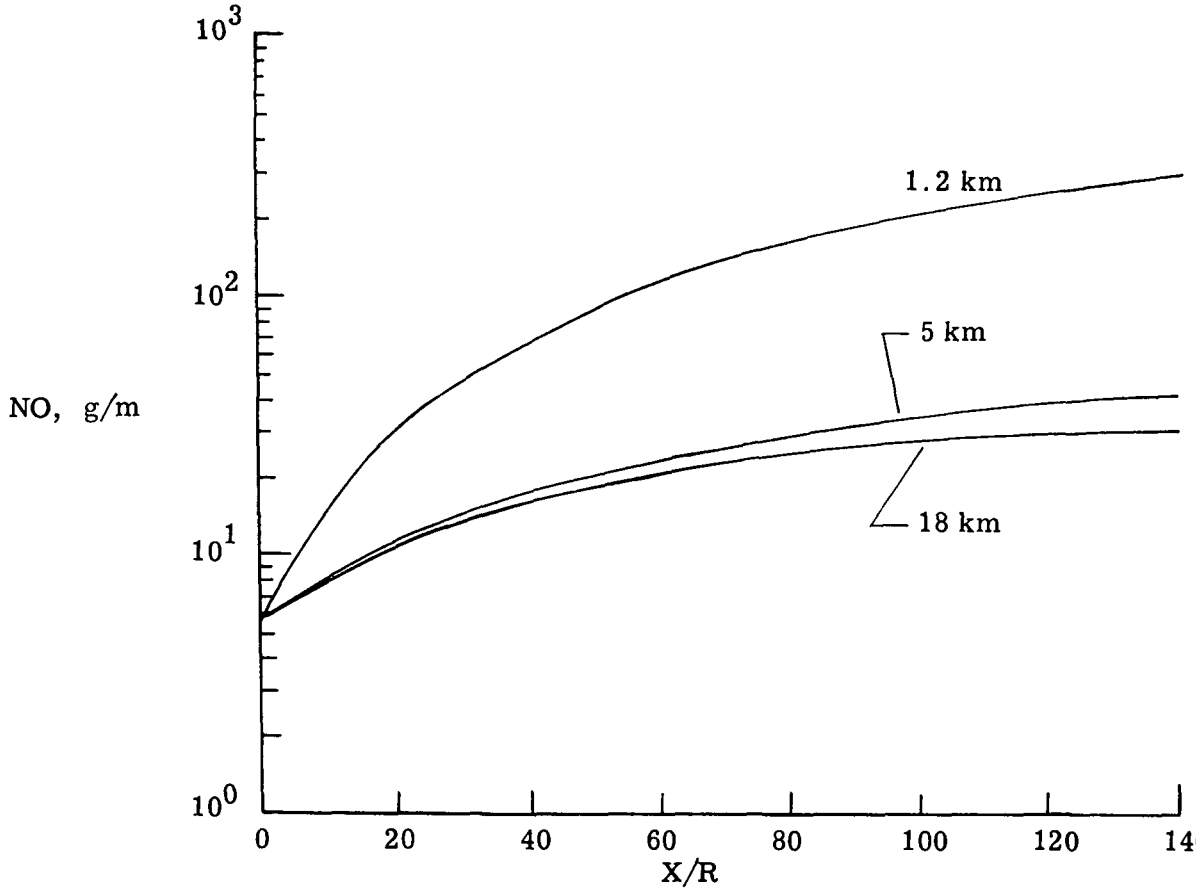

Figure 4.- NO production for the Titan III-C at three altitudes.

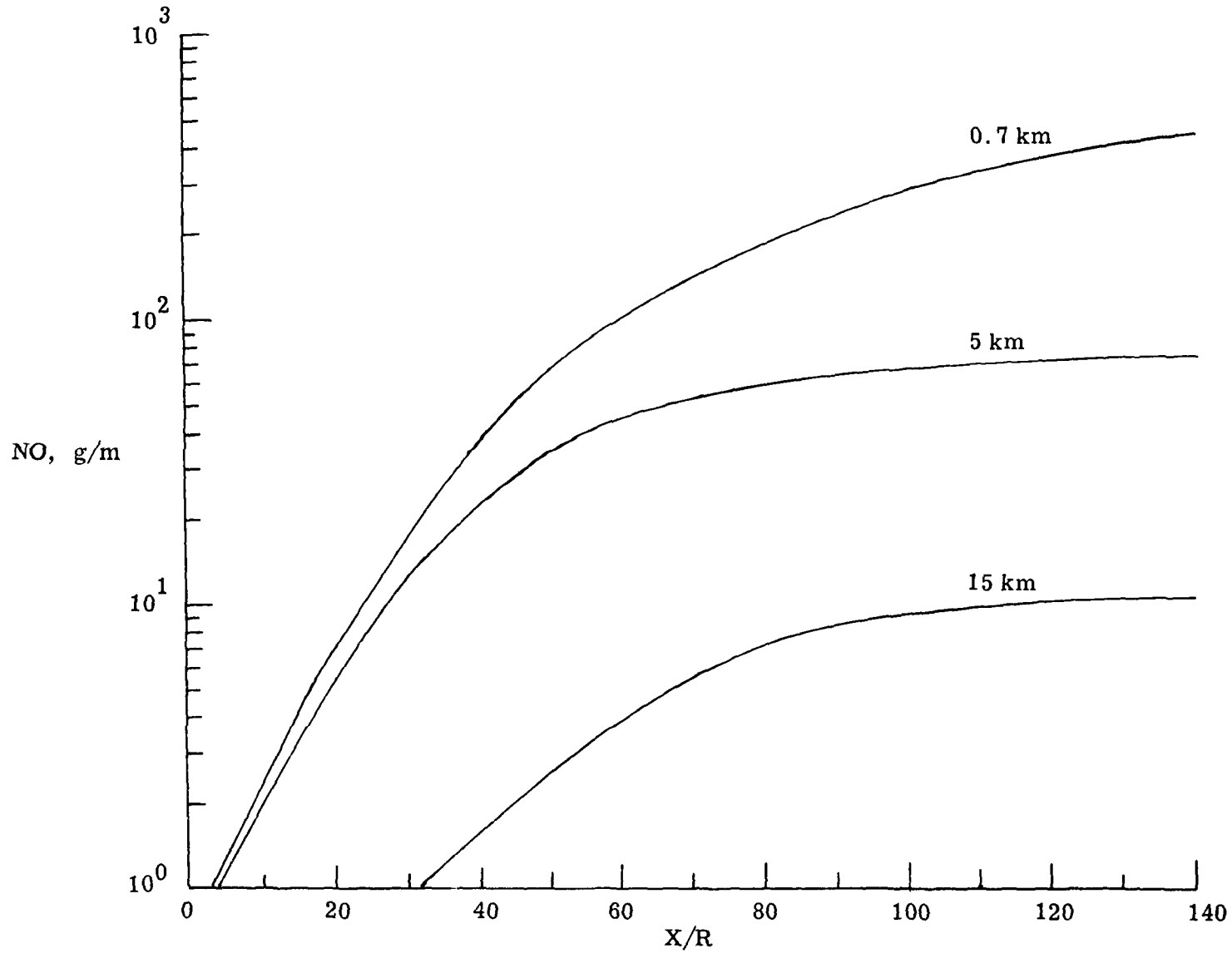

Figure 5.- NO production for shuttle at three altitudes.

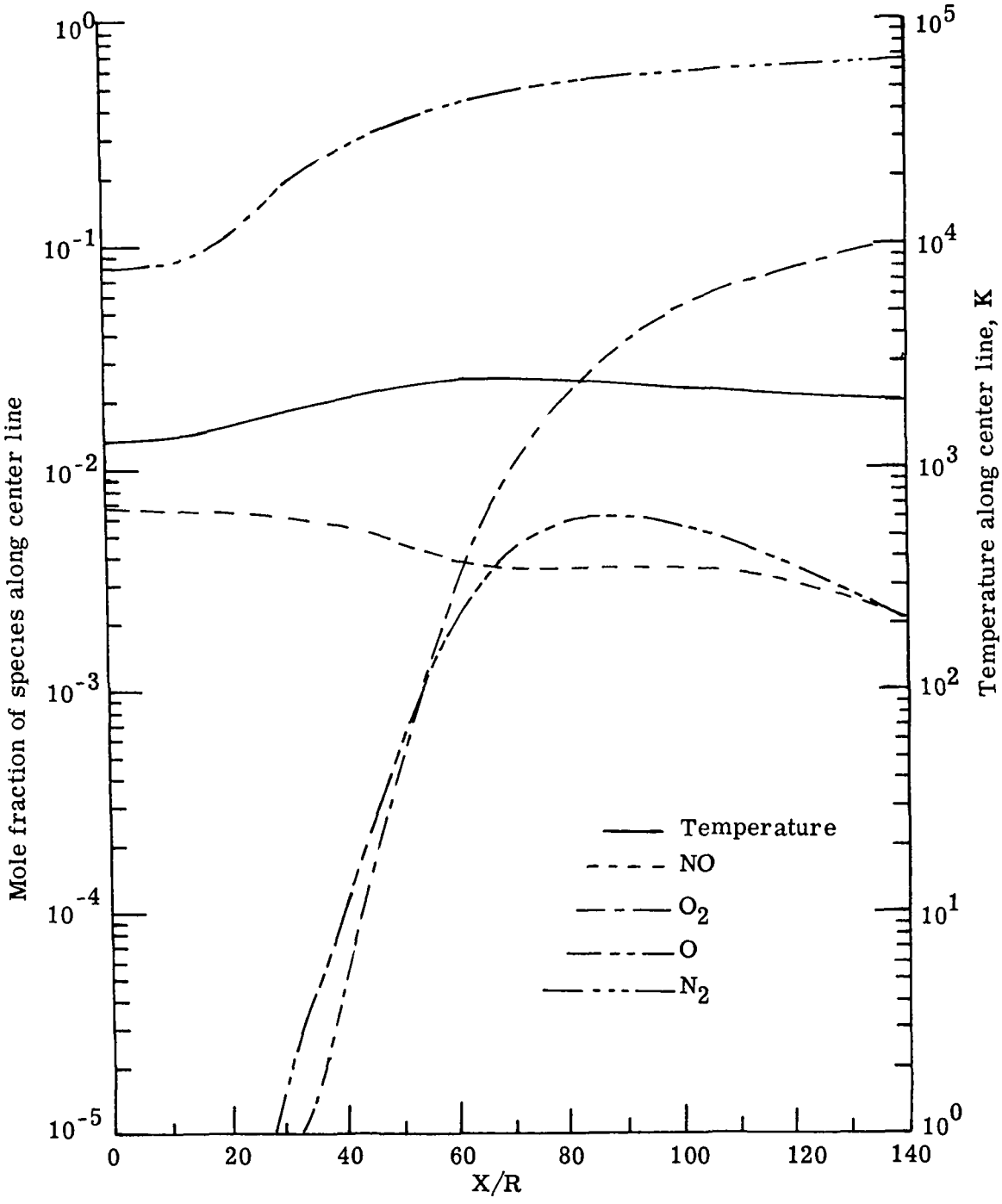

Figure 6.- Center-line mole fractions and temperature as function of downstream distance for plume of a Titan III-C motor at an altitude of 18 km with thrust vector control.

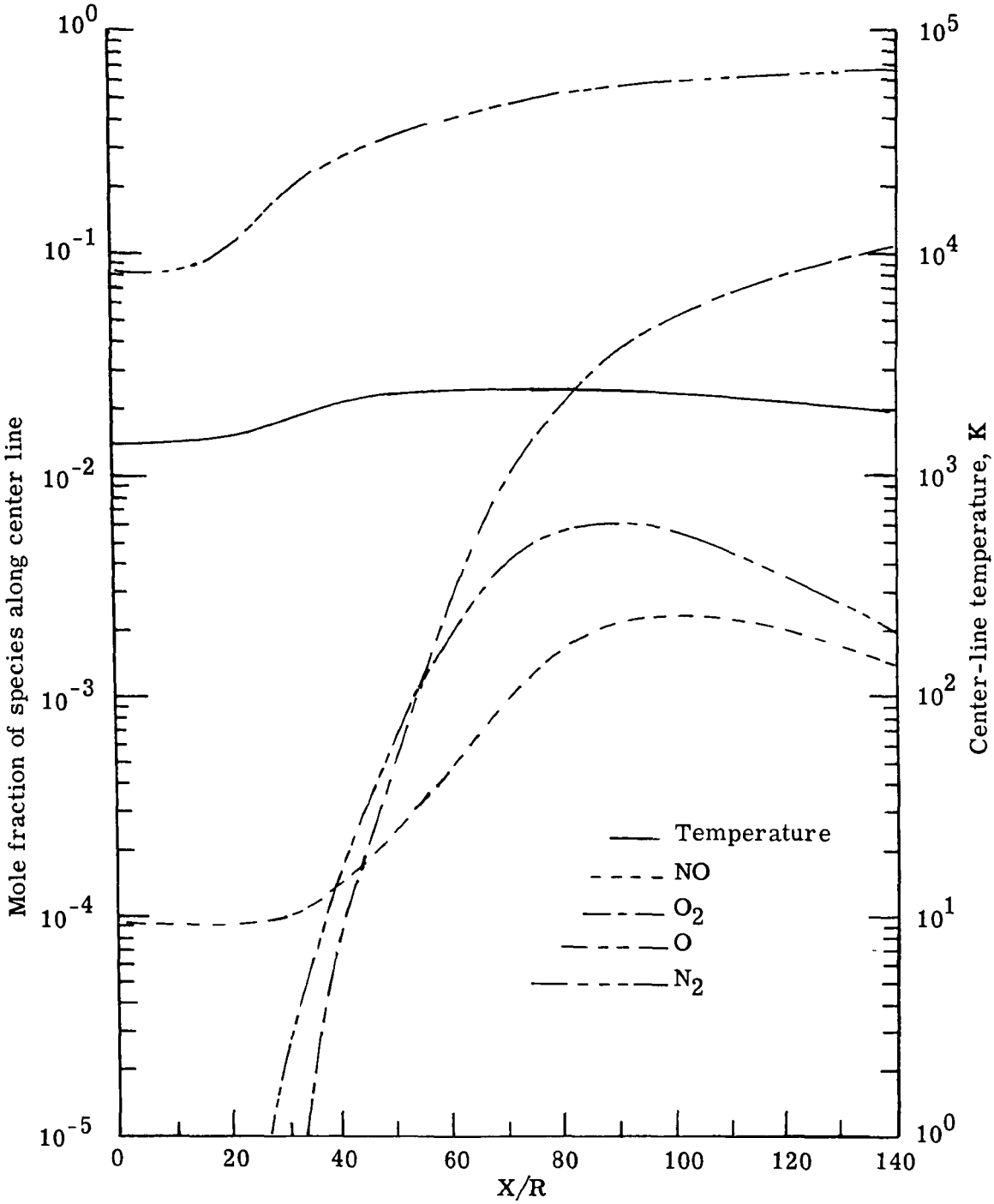

Figure 7.- Center-line mole fractions and temperature as function of downstream distance for plume of a Titan III-C motor at an altitude of 18 km without thrust vector control.

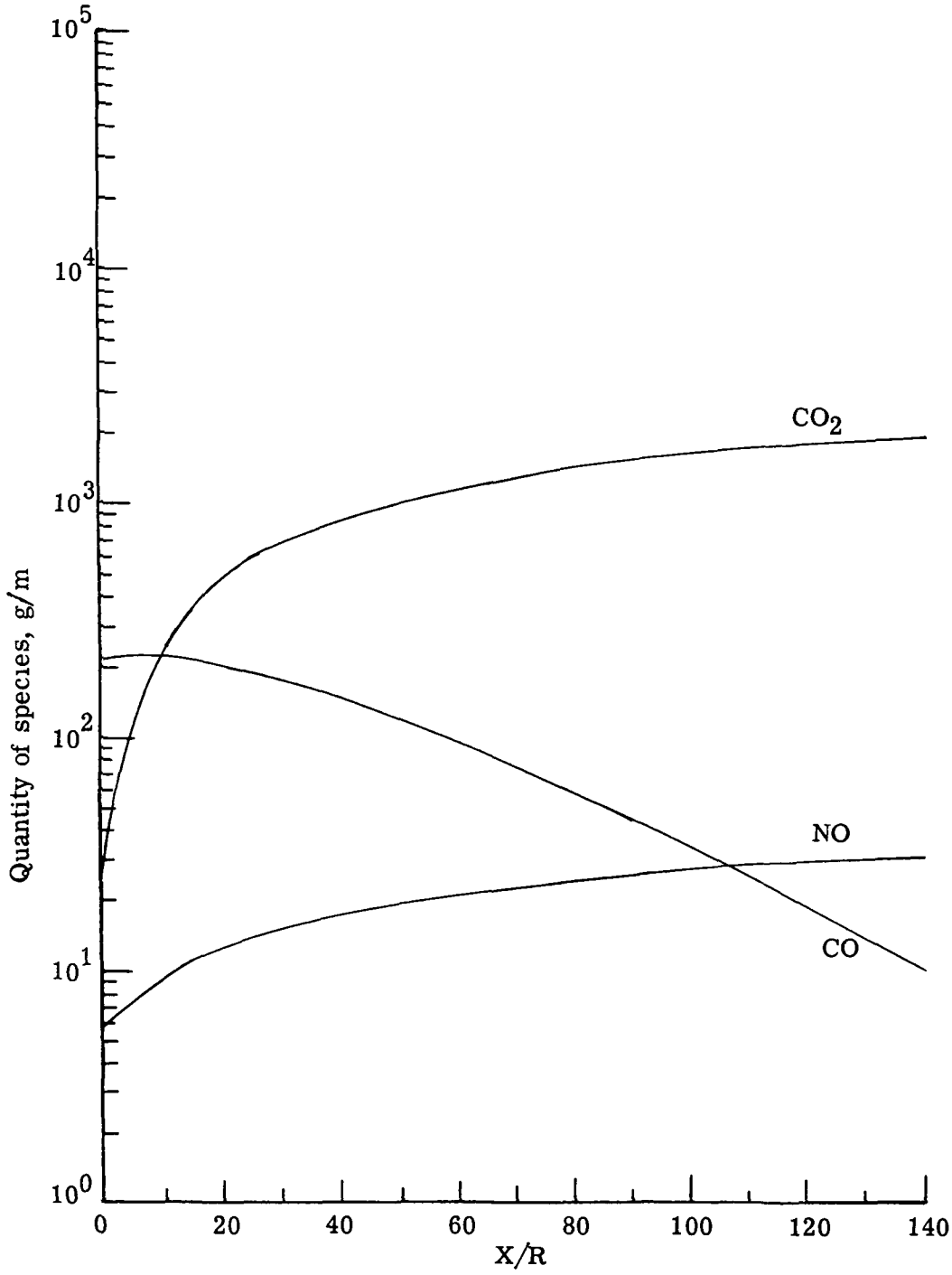

Figure 8.- Amount of species produced by a Titan III-C motor as function of downstream distance at an altitude of 18 km with thrust vector control.

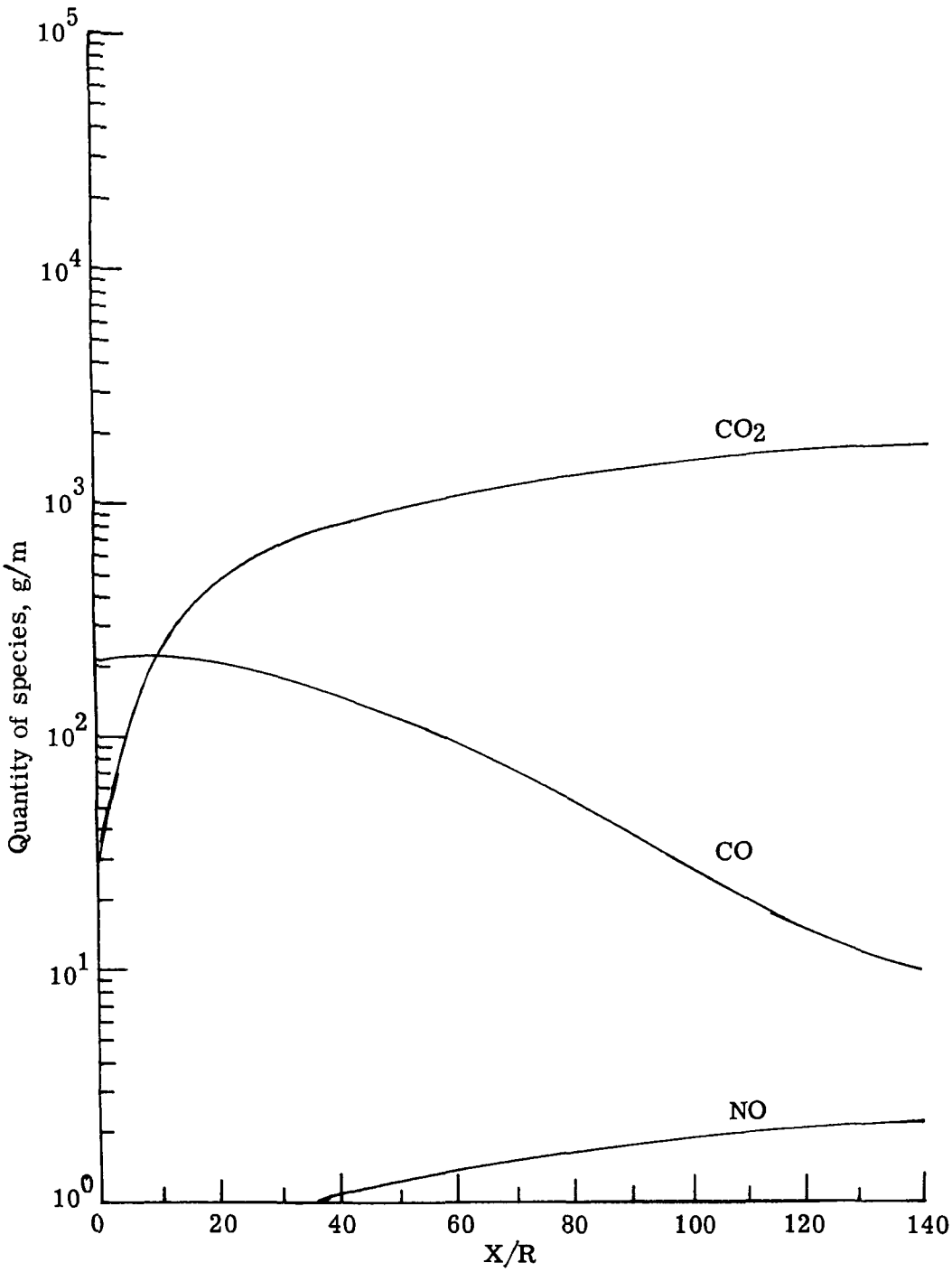

Figure 9.- Amount of species produced by a Titan III-C motor as function of downstream distance at an altitude of 18 km without thrust vector control.

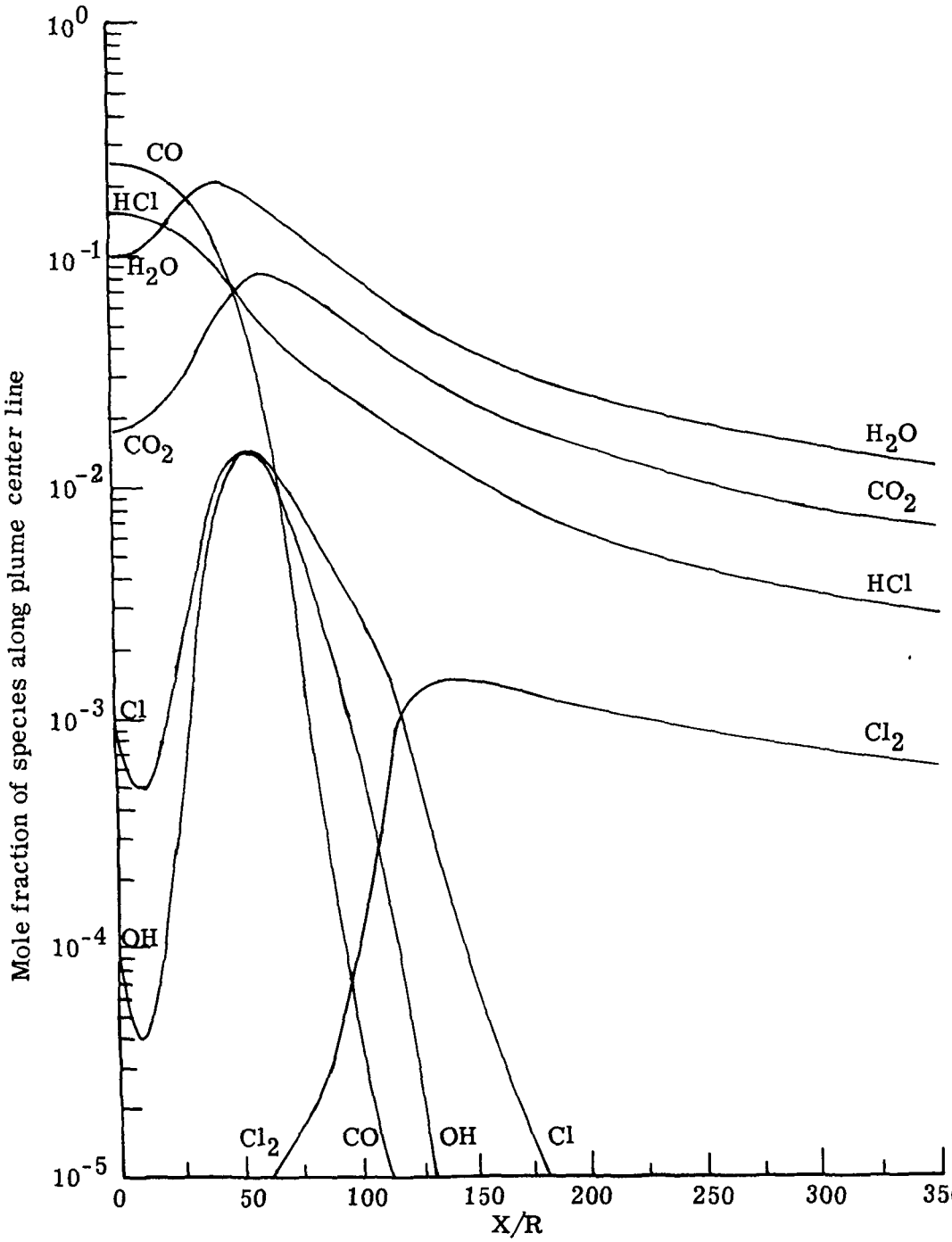

Figure 10.- Center-line mole fractions of species appropriate to combustion as function of downstream distance for a Titan III-C motor at an altitude of 1.2 km.

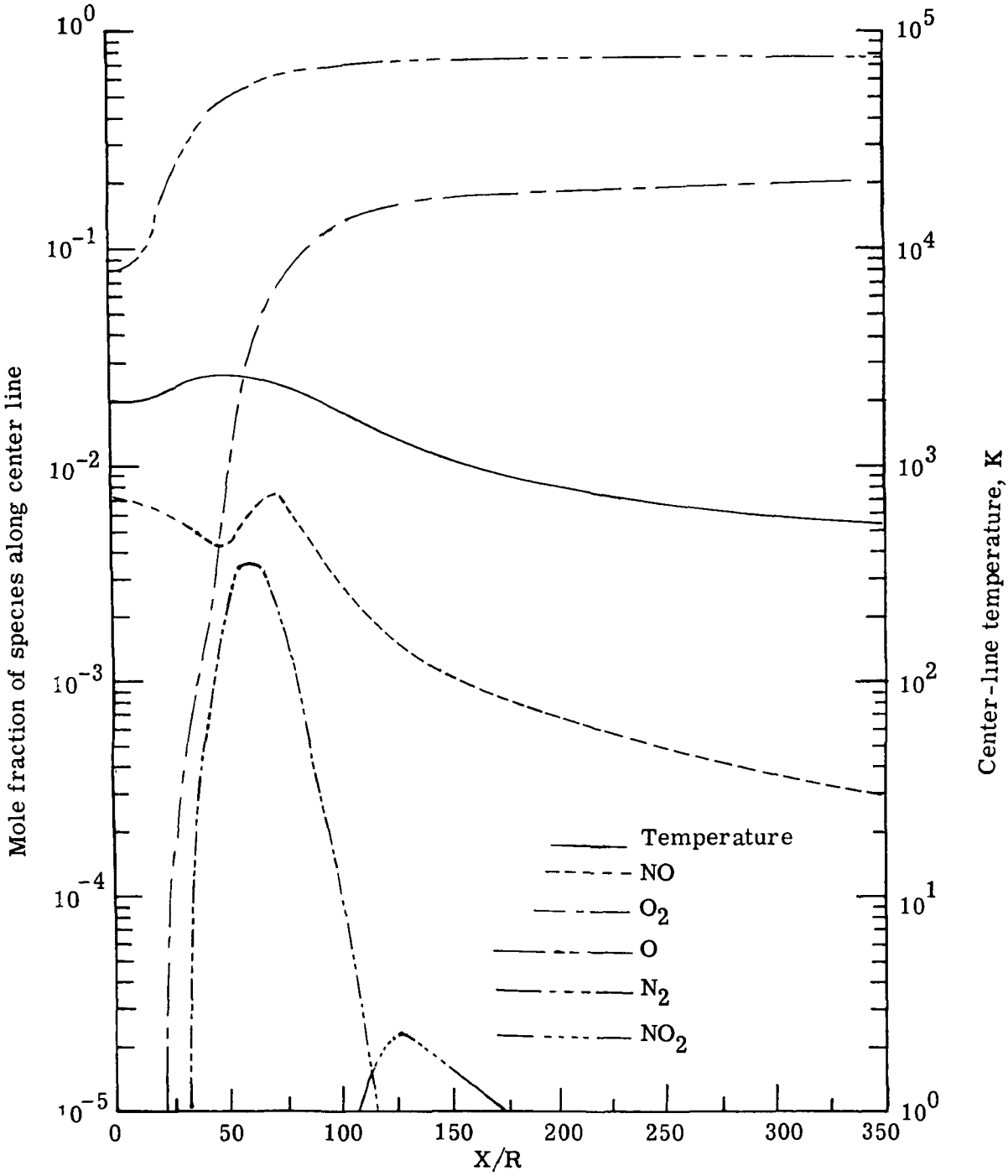

Figure 11.- Center-line mole fractions and temperature as function of downstream distance for plume of Titan III-C motor at an altitude of 1.2 km.

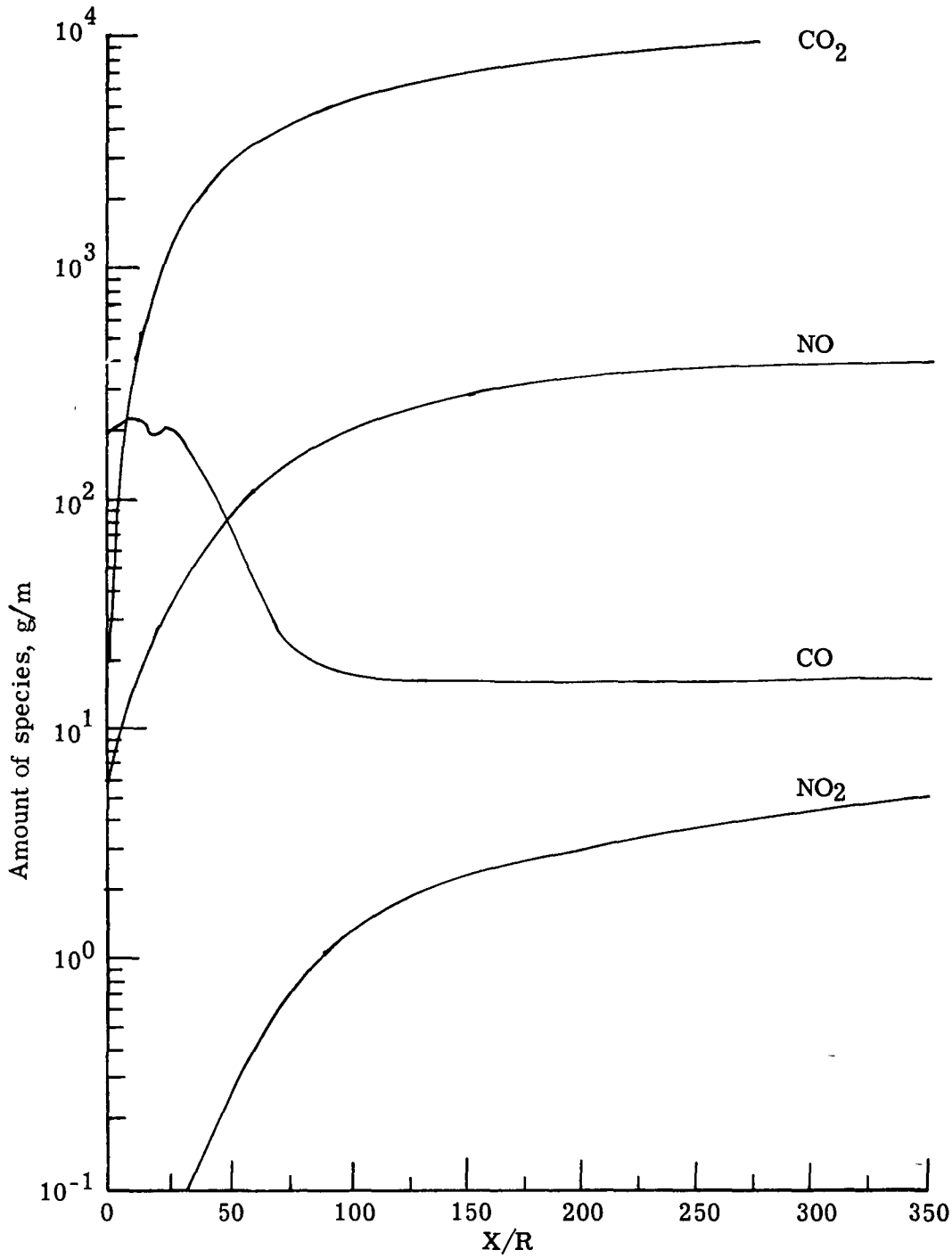

Figure 12.- Amount of species produced in plume of a Titan III-C motor as function of downstream distance at an altitude of 1.2 km.

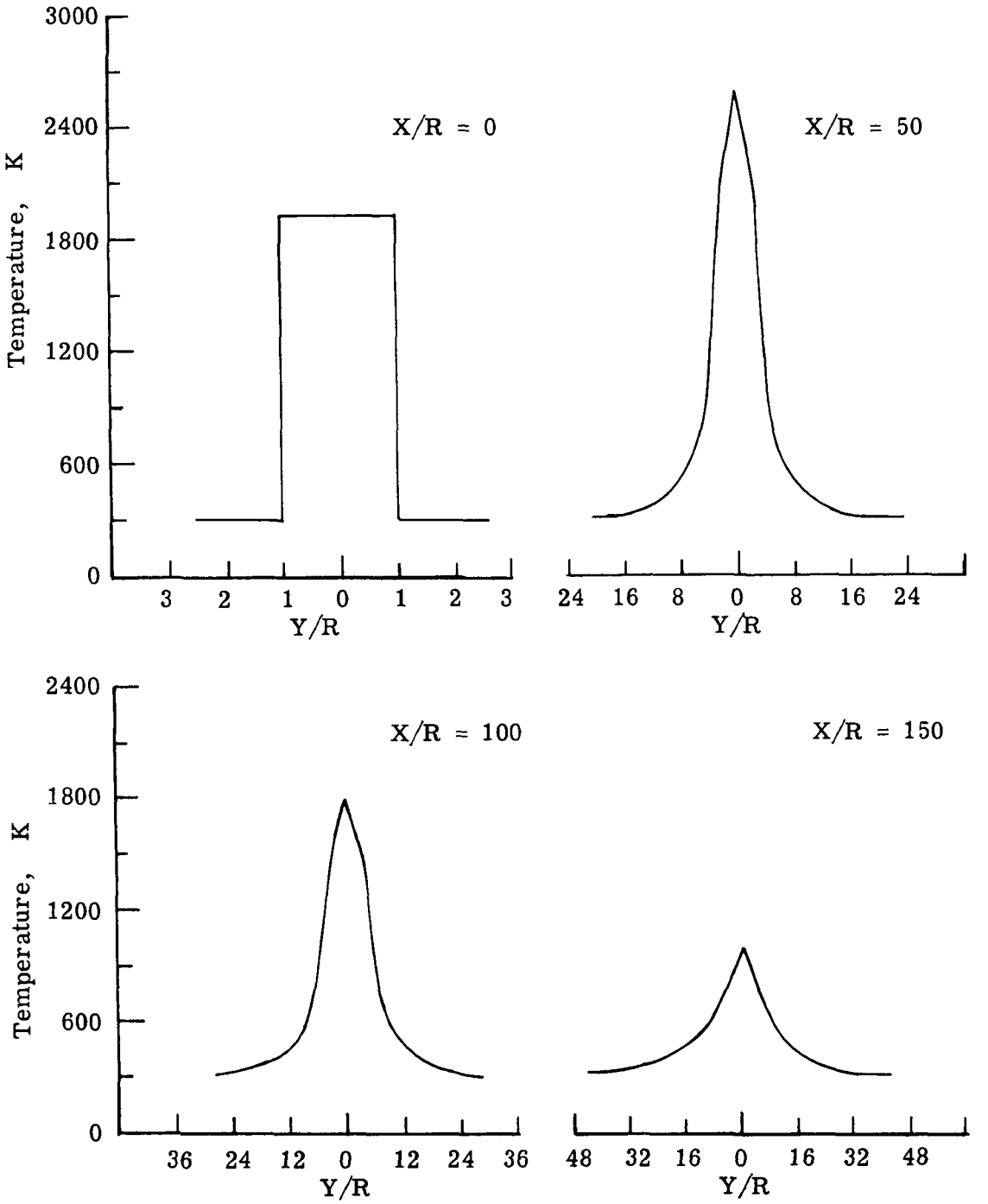

Figure 13.- Cross-sectional temperature profiles at various downstream distances for a Titan III-C at 1.2 km.

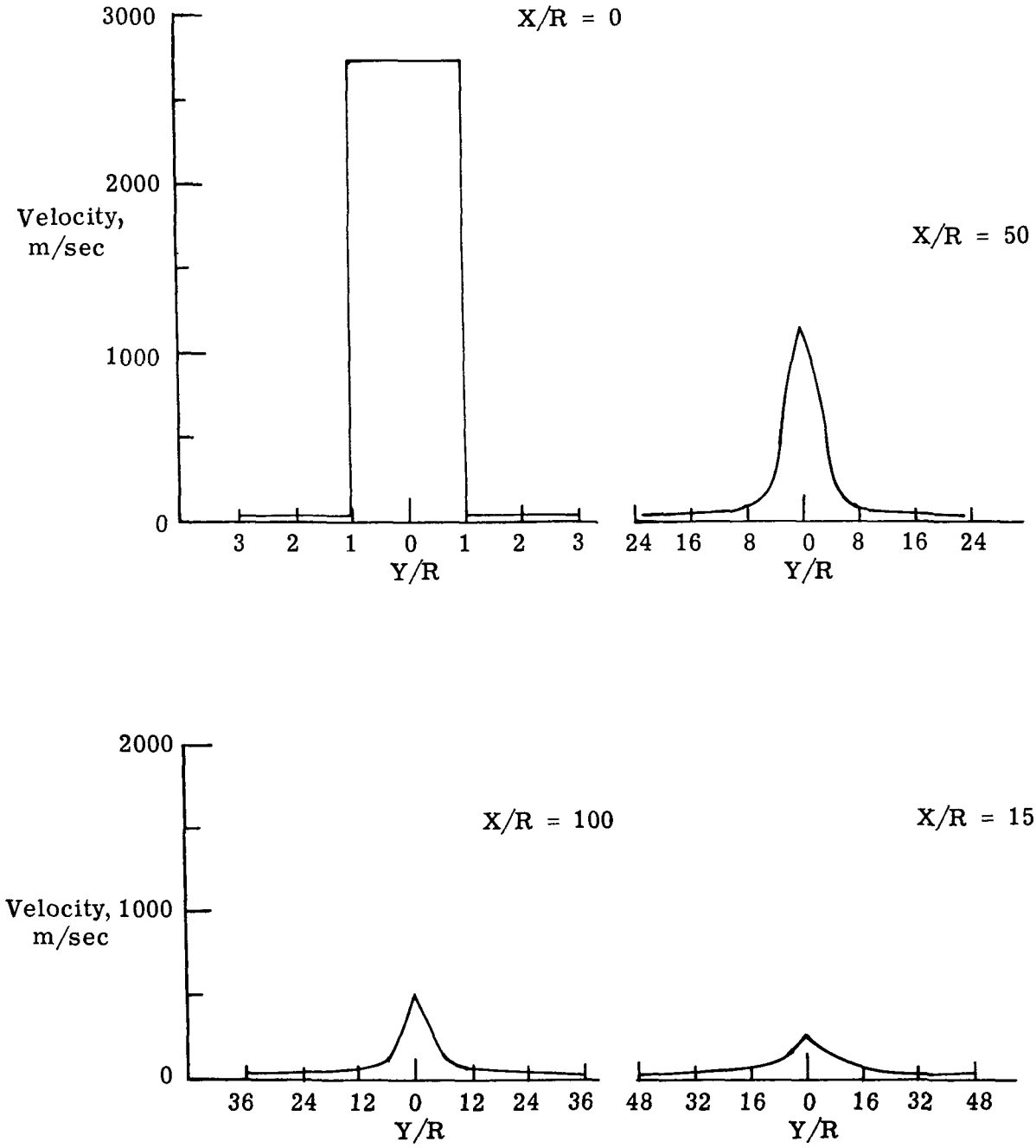

Figure 14.- Cross-sectional velocity profiles at various downstream distances for a Titan III-C at 1.2 km.

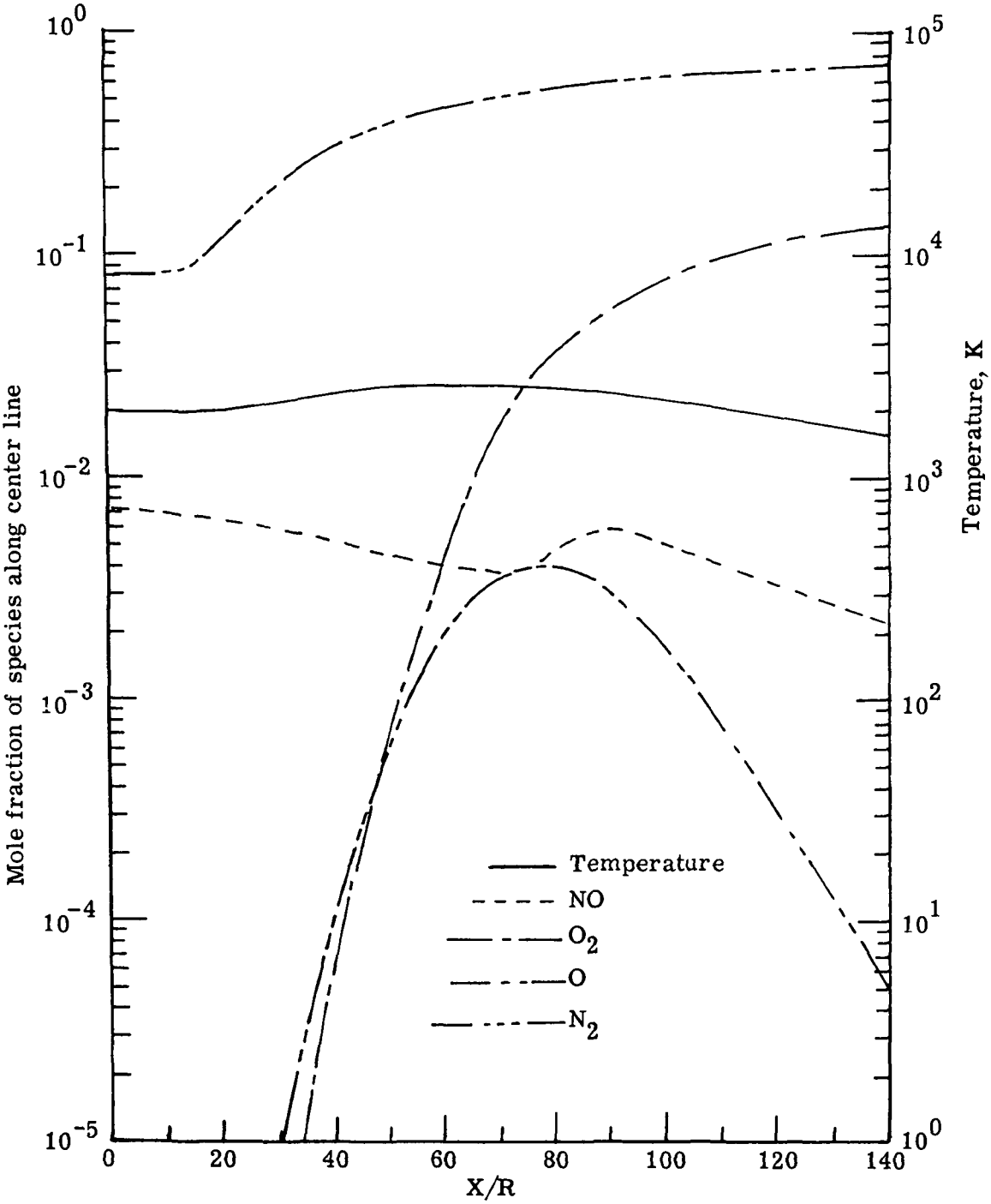

Figure 15.- Center-line mole fractions and temperatures as functions of downstream distance for plume of a Titan III-C motor at an altitude of 5 km.

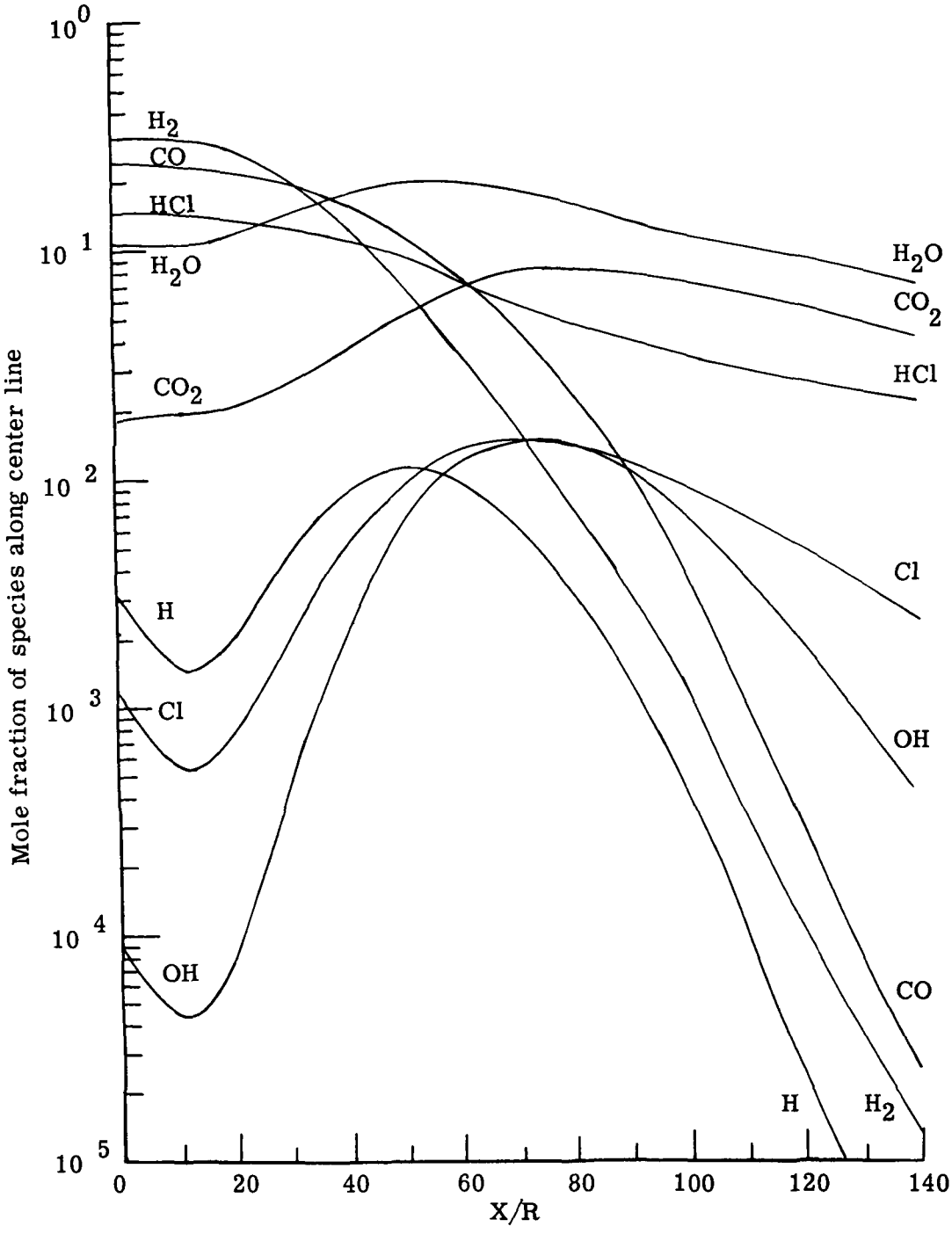

Figure 16.- Center-line mole fractions of species appropriate to combustion as function of downstream distances for plume of a Titan III-C motor at an altitude of 5 km.

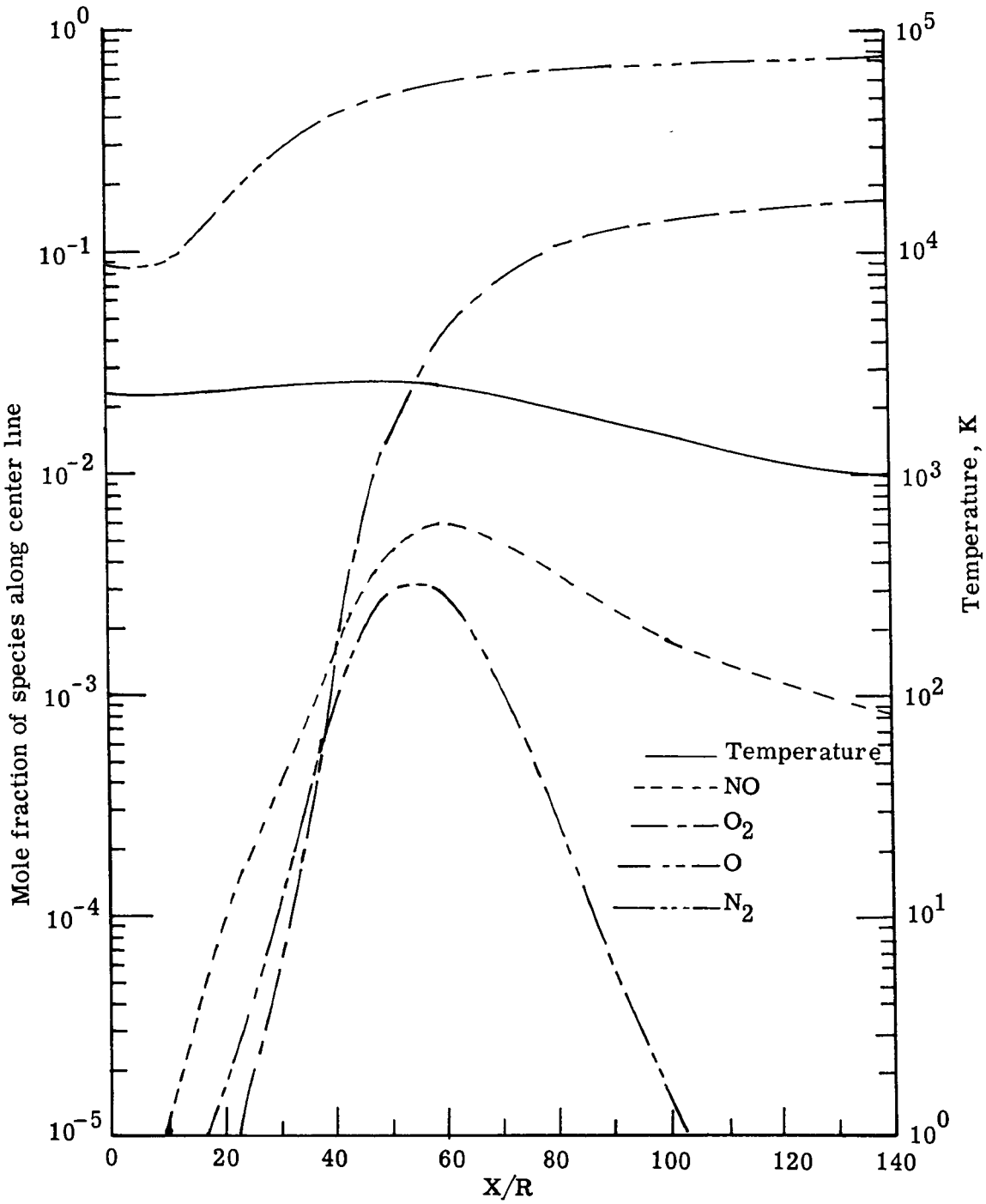

Figure 17.- Center-line mole fractions and temperature as functions of downstream distance for plume of a shuttle motor at an altitude of 0.7 km.

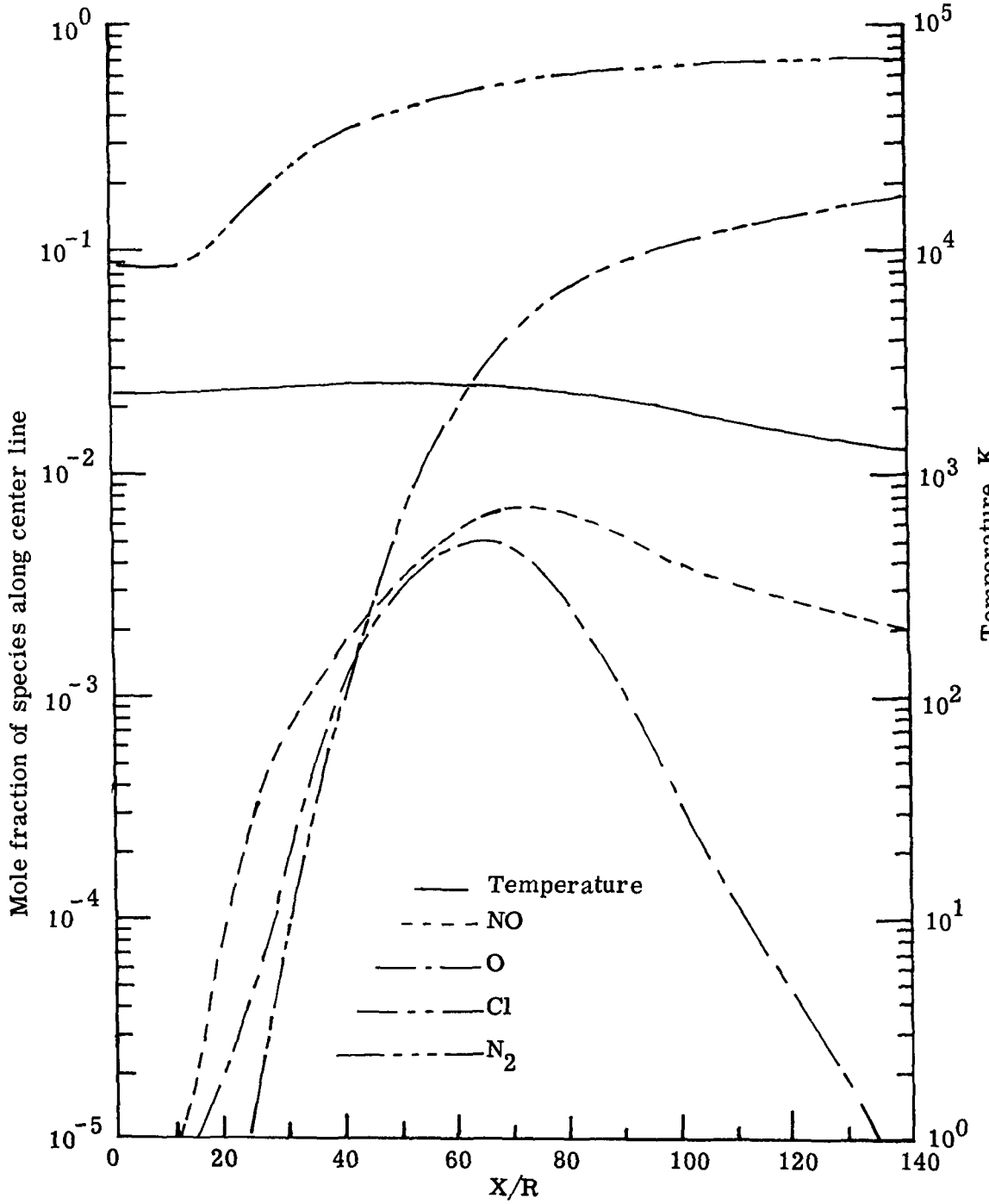

Figure 18.- Center-line mole fractions and temperature as functions of downstream distance for plume of a shuttle motor at an altitude of 5 km.

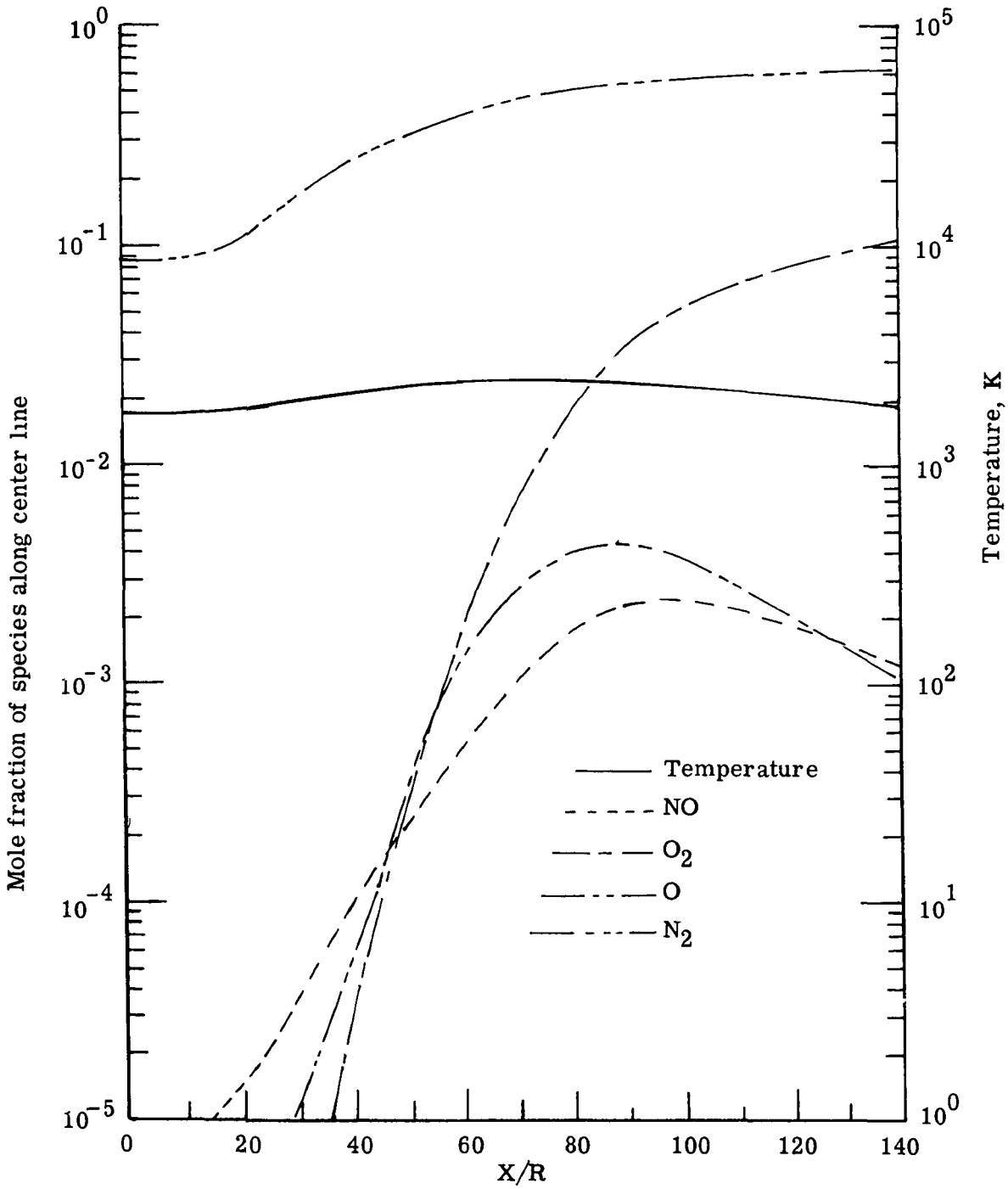

Figure 19.- Center-line mole fractions and temperature as functions of downstream distance for plume of a shuttle motor at an altitude of 15 km.

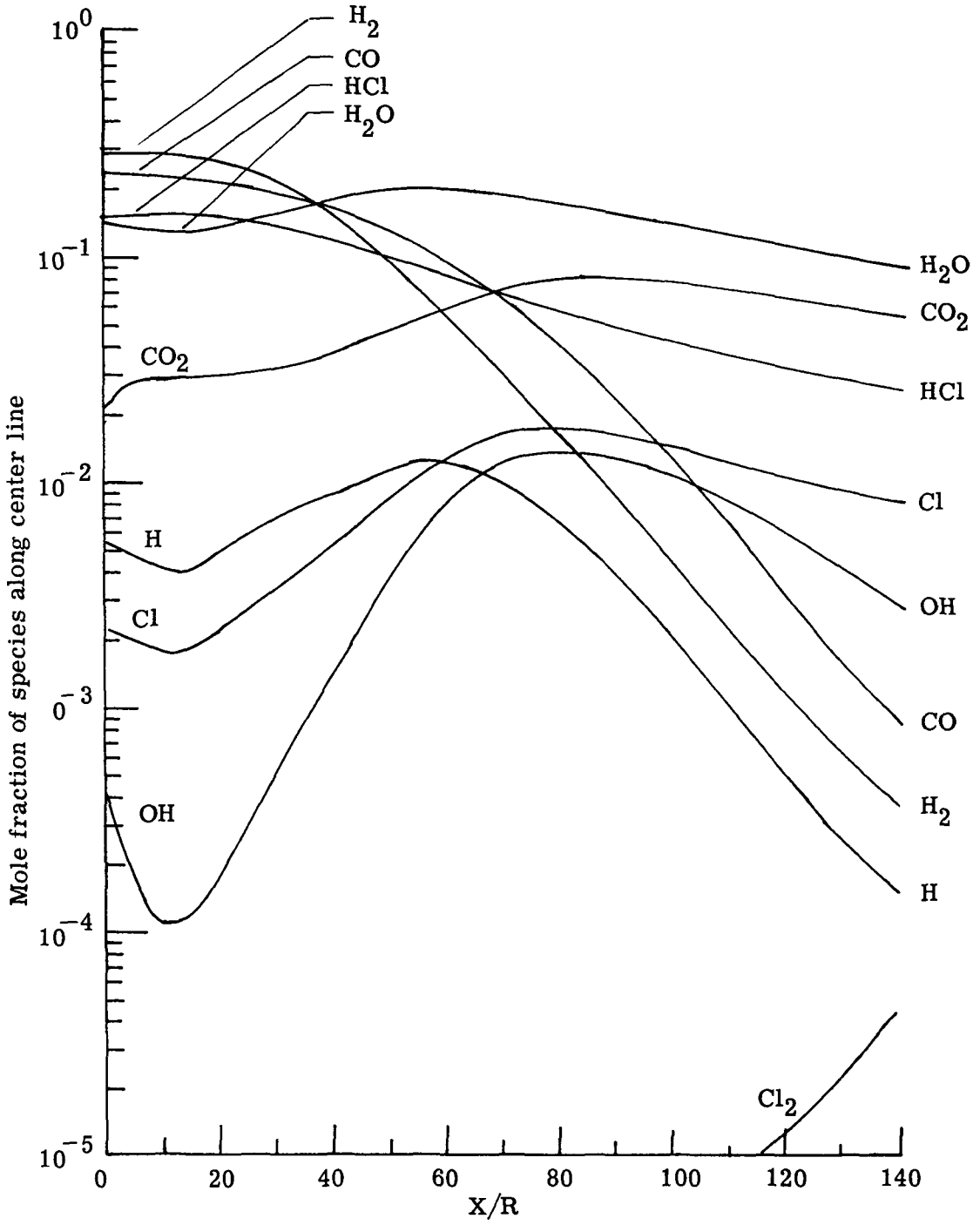

Figure 20.- Center-line mole fractions of species appropriate to combustion as function of downstream distance for plume of a shuttle motor at an altitude of 0.7 km.

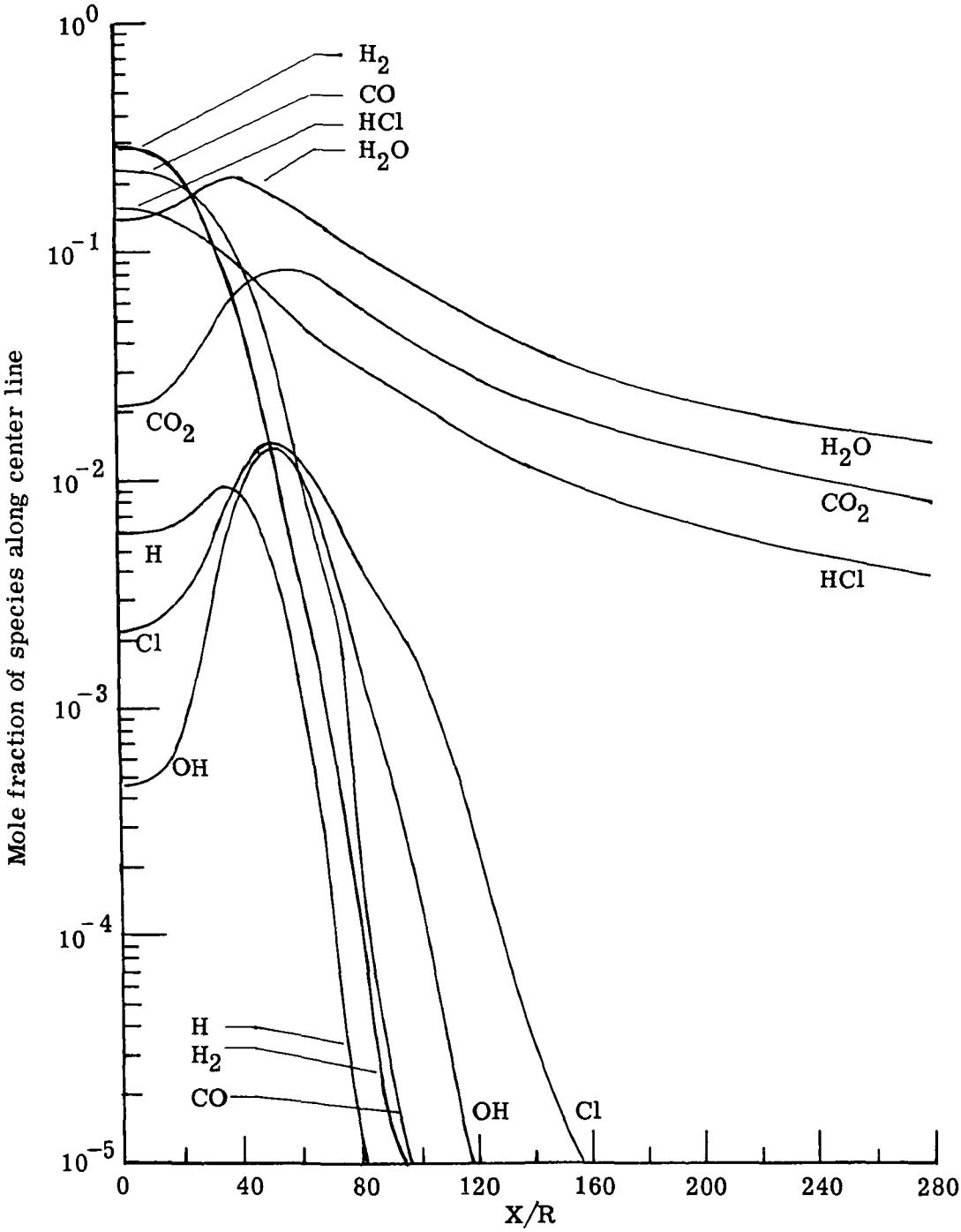

Figure 21.- Center-line mole fractions of species appropriate to combustion as function of downstream distance in plume of a shuttle motor at an altitude of 15 km.

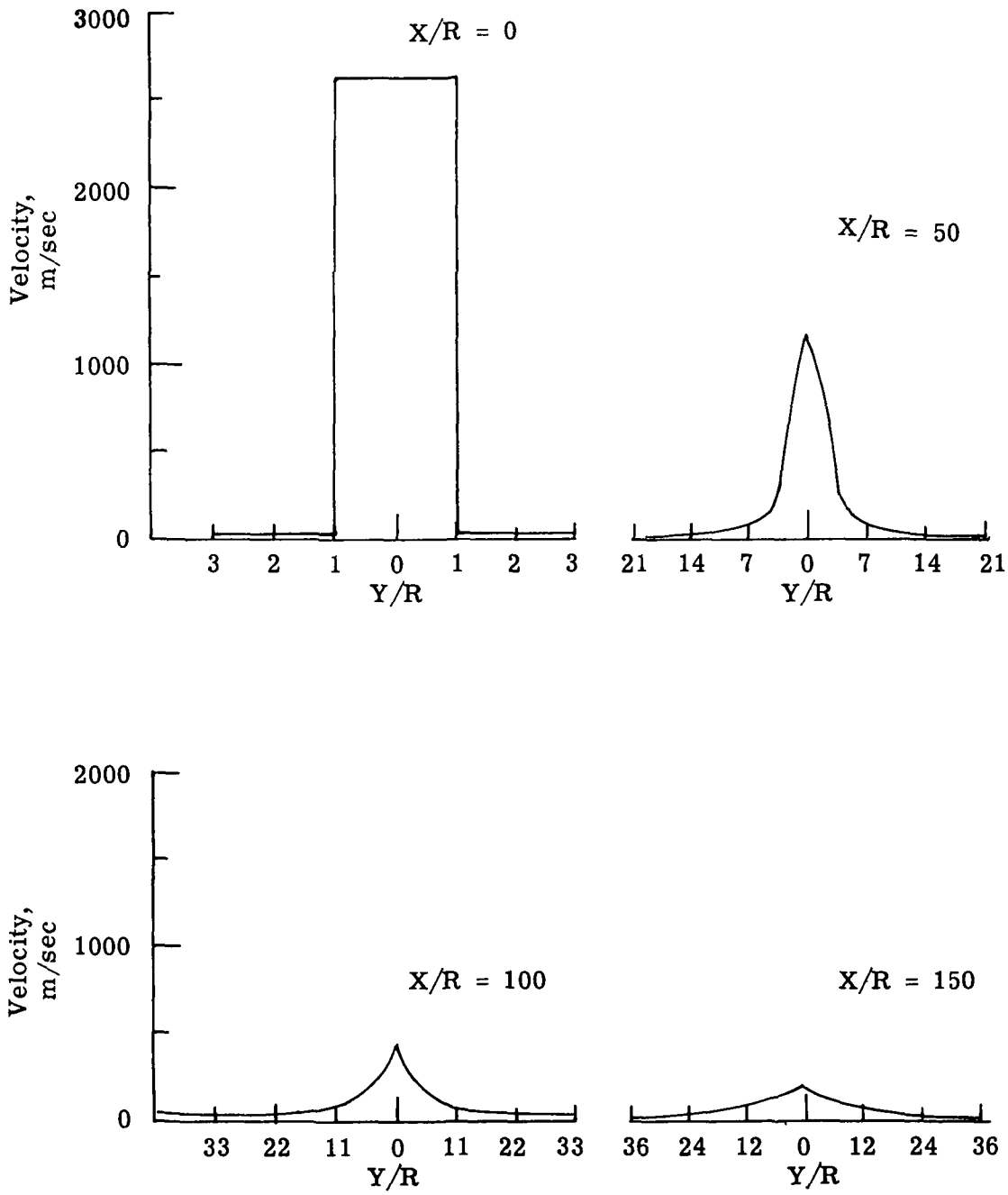

Figure 22.- Cross-sectional velocity profiles at various downstream distances from a shuttle motor at an altitude of 0.7 km.

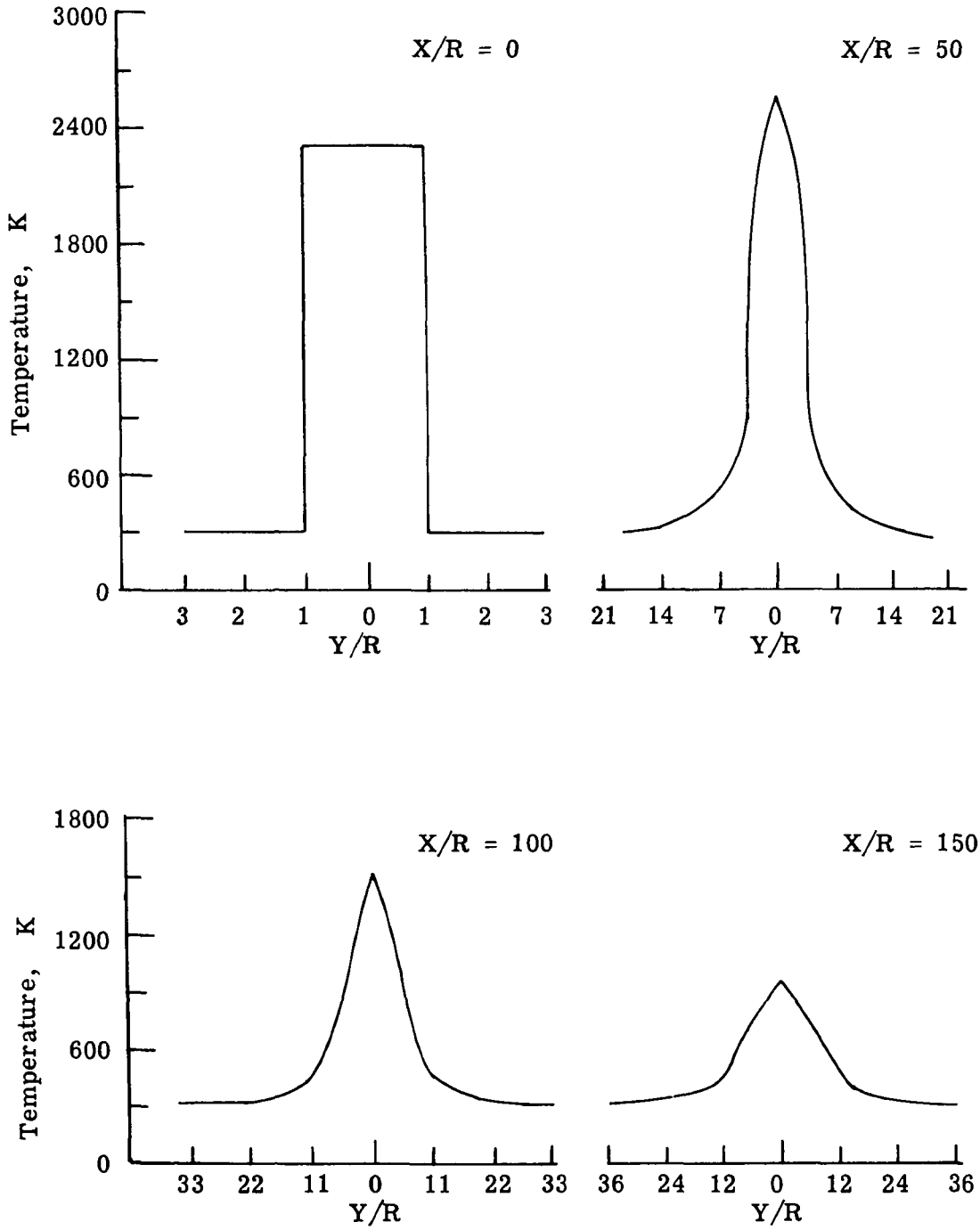

Figure 23.- Cross-sectional temperature profiles at various downstream distances from a shuttle motor at an altitude of 0.7 km.

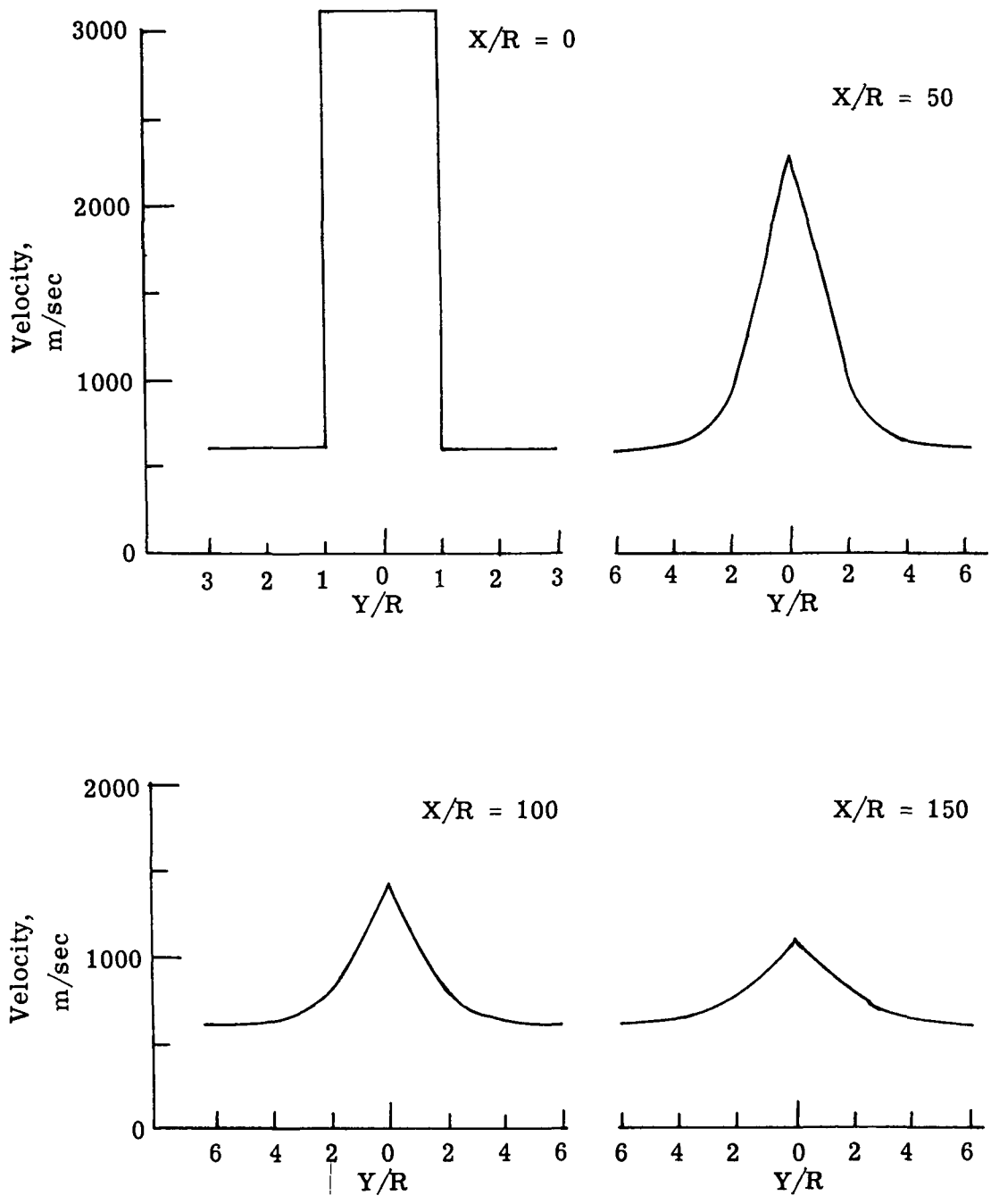

Figure 24.- Cross-sectional velocity profiles at various downstream distances from a shuttle motor at an altitude of 15 km.

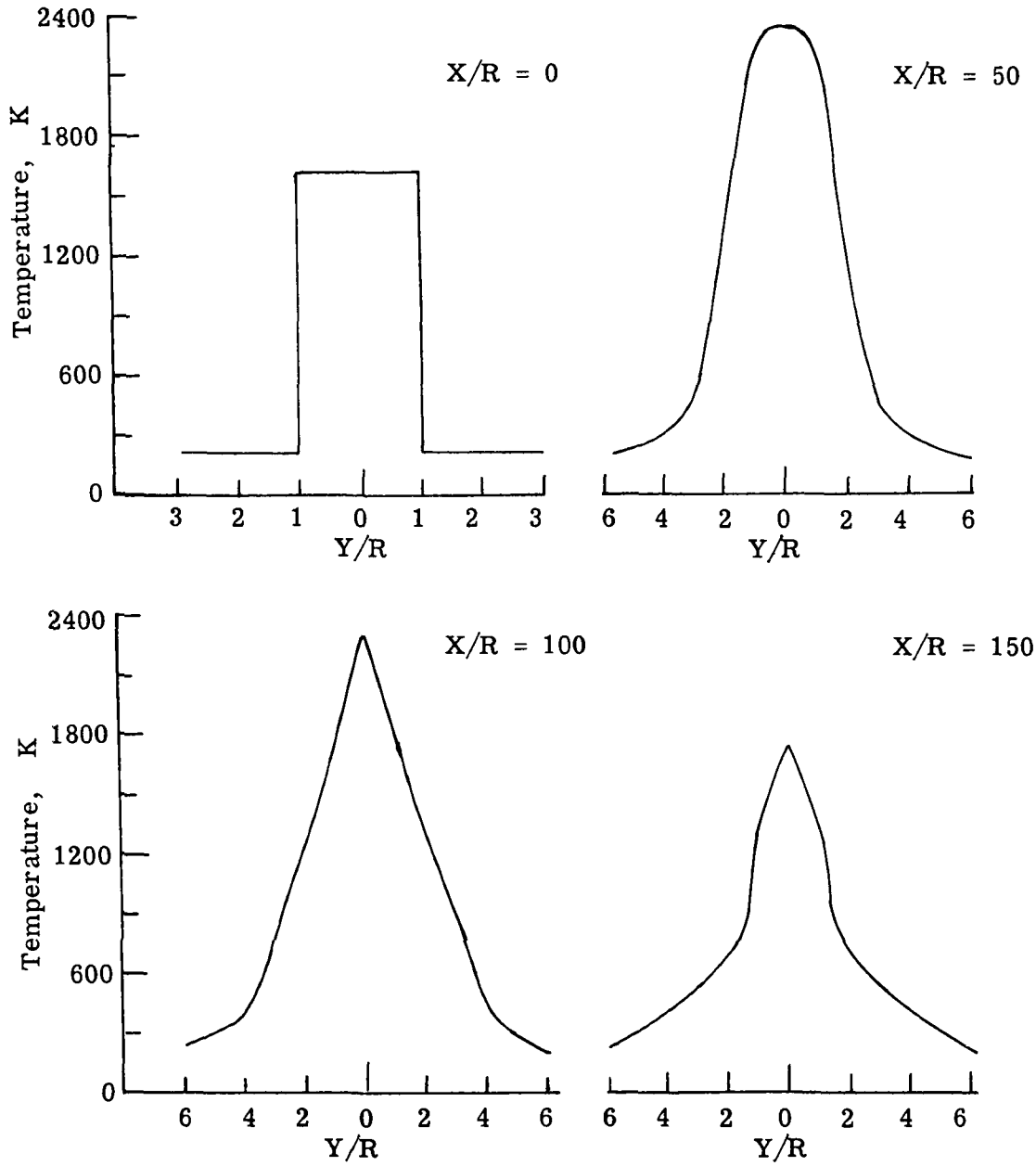

Figure 25.- Cross-sectional temperature profiles at various downstream distances from a shuttle motor at an altitude of 15 km.

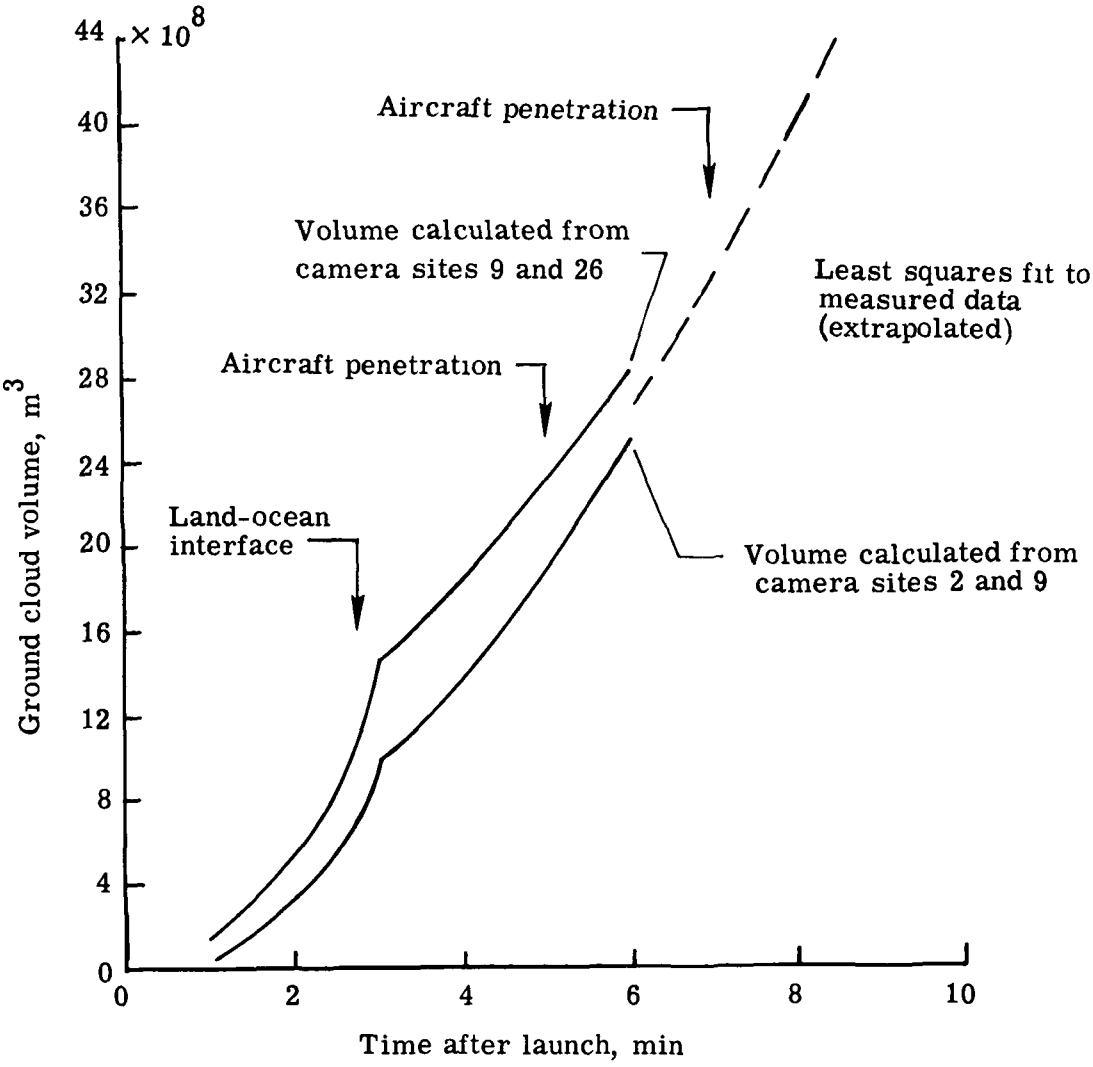

Figure 26.- Ground cloud volume as a function of time.

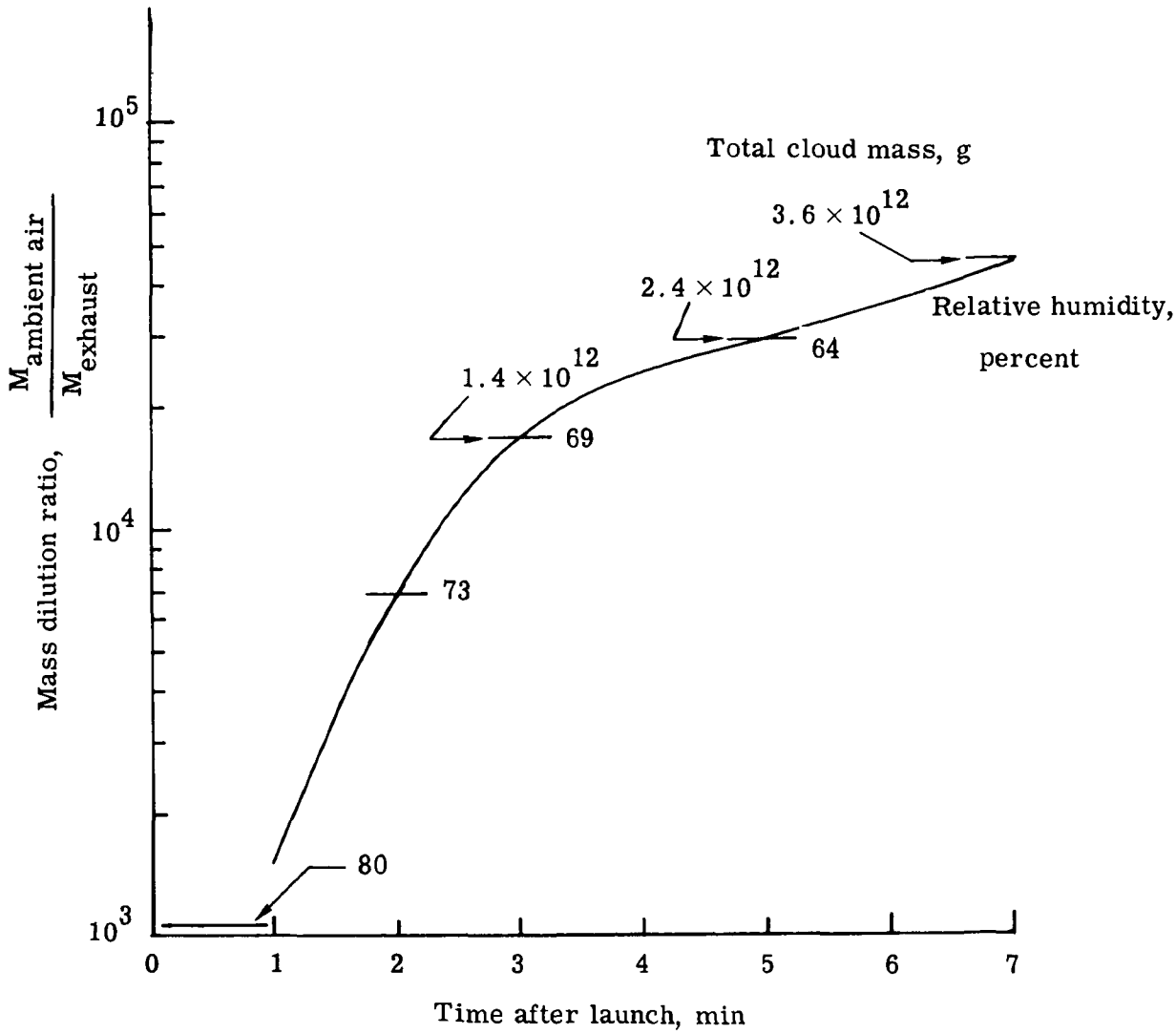

Figure 27.- Ground cloud mass and mass dilution ratio as a function of time.

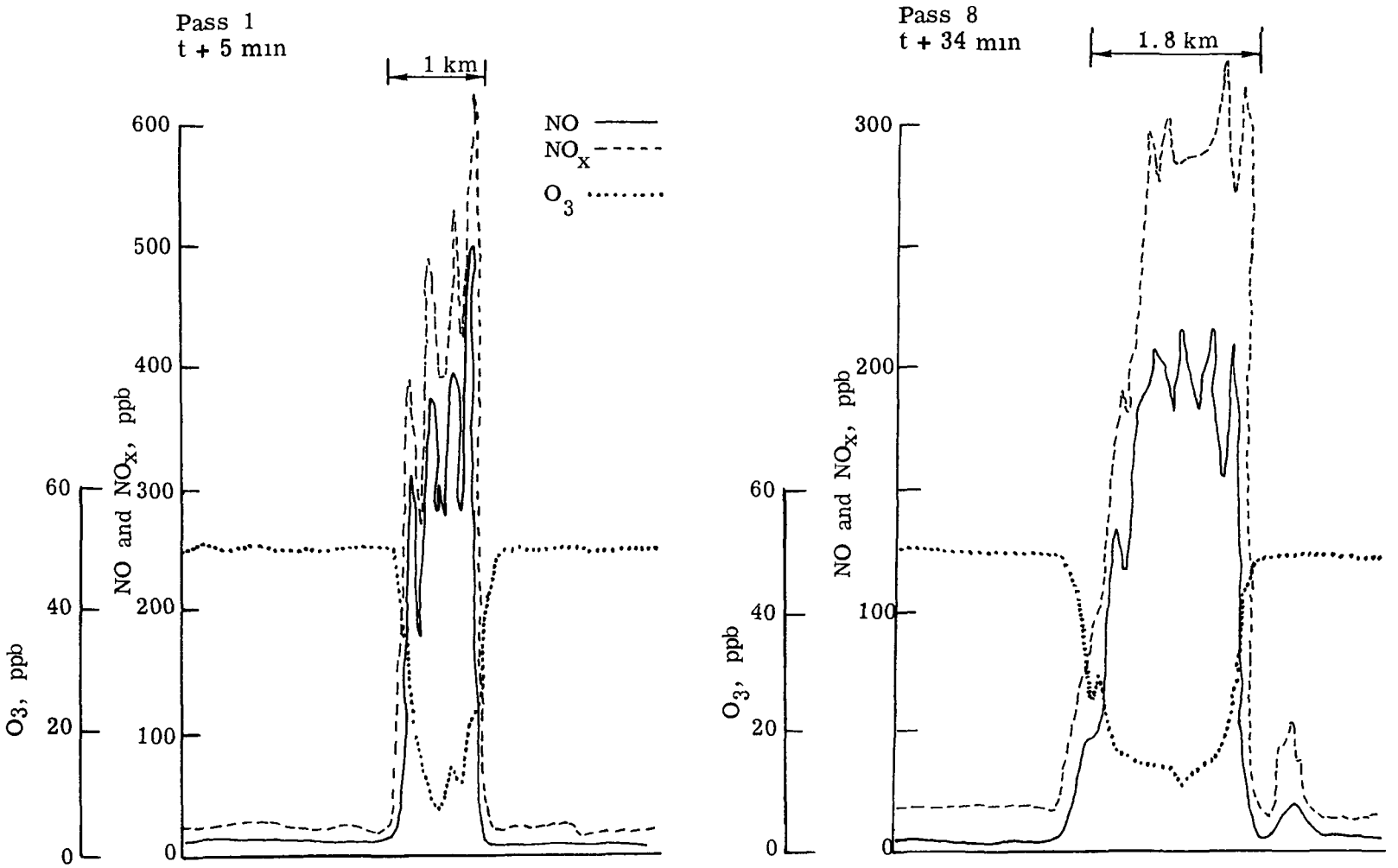

Figure 28.- Aircraft data traces at t + 5 min and t + 34 min.

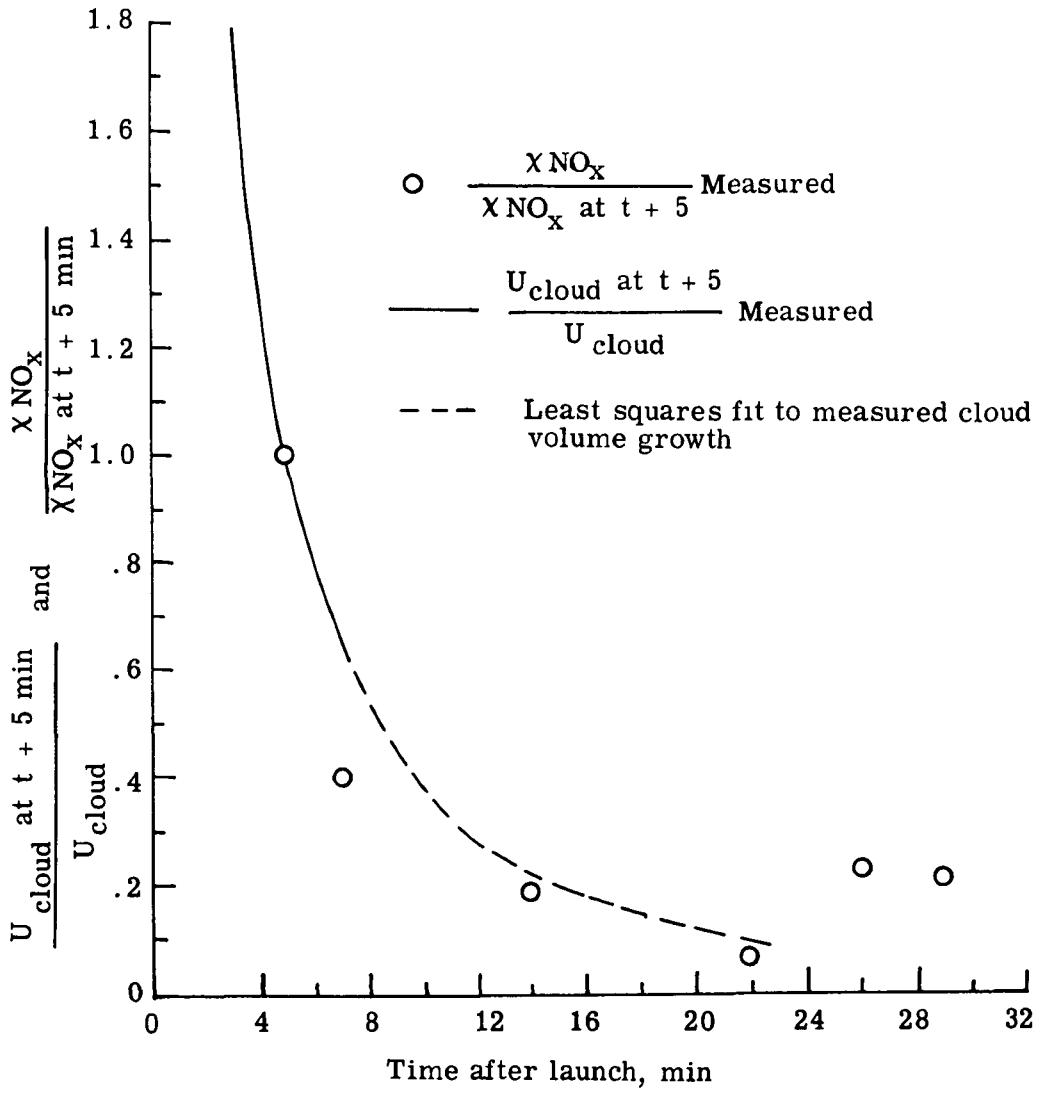

Figure 29.- Ground cloud NO_x concentration as a function of time.

NATIONAL AERONAUTICS AND SPACE ADMINISTRATION
WASHINGTON, D C 20546

OFFICIAL BUSINESS
PENALTY FOR PRIVATE USE $300

SPECIAL FOURTH-CLASS RATE BOOK

POSTAGE AND FEES PAID
NATIONAL AERONAUTICS AND SPACE ADMINISTRATION
451

U.S.MAIL

POSTMASTER If Undeliverable (Section 158 Postal Manual) Do Not Return

"The aeronautical and space activities of the United States shall be conducted so as to contribute . to the expansion of human knowledge of phenomena in the atmosphere and space The Administration shall provide for the widest practicable and appropriate dissemination of information concerning its activities and the results thereof"

—NATIONAL AERONAUTICS AND SPACE ACT OF 1958

NASA SCIENTIFIC AND TECHNICAL PUBLICATIONS

TECHNICAL REPORTS Scientific and technical information considered important, complete, and a lasting contribution to existing knowledge

TECHNICAL NOTES Information less broad in scope but nevertheless of importance as a contribution to existing knowledge

TECHNICAL MEMORANDUMS Information receiving limited distribution because of preliminary data, security classification, or other reasons Also includes conference proceedings with either limited or unlimited distribution.

CONTRACTOR REPORTS Scientific and technical information generated under a NASA contract or grant and considered an important contribution to existing knowledge

TECHNICAL TRANSLATIONS Information published in a foreign language considered to merit NASA distribution in English

SPECIAL PUBLICATIONS Information derived from or of value to NASA activities. Publications include final reports of major projects, monographs, data compilations, handbooks, sourcebooks, and special bibliographies

TECHNOLOGY UTILIZATION PUBLICATIONS Information on technology used by NASA that may be of particular interest in commercial and other non-aerospace applications Publications include Tech Briefs, Technology Utilization Reports and Technology Surveys

Details on the availability of these publications may be obtained from:

SCIENTIFIC AND TECHNICAL INFORMATION OFFICE

NATIONAL AERONAUTICS AND SPACE ADMINISTRATION

Washington, D.C. 20546